DOI: 10.1002/asia.201000545

Highly Efficient and Directional Homo- and Heterodimeric Energy Transfer Materials Based on Fluorescently Derivatized α,γ-Cyclic Octapeptides

Roberto J. Brea,[a] María Jesús Pérez-Alvite,[a] Michele Panciera,[a] Manuel Mosquera,[b] Luis Castedo,[a] and Juan R. Granja*[a]

Abstract: Cyclic octapeptides composed of α-amino acids alternated with *cis*-3-aminocycloalkanecarboxylic acids, self-assemble as drumlike dimers through β-sheet-like, backbone-to-backbone hydrogen bonding. Heterodimerization appears to be significantly more favored than homodimerization, and this represents a novel approach for the design and fabrication of highly stable heterodimeric assemblies. A multicomponent equilibrium network based on fluorescently derivatized self-assembling α,γ-cyclic octapeptides has been successfully used to form light-harvesting/light-converting ensembles with a distinctive organization of donor and acceptor units able to act as efficient artificial photosystems.

Keywords: amino acids · cyclic peptides · FRET · heterodimers · self-assembly

Introduction

Natural photosynthesis provides an efficient example of the hierarchical organization in space of a multitude of chromophoral molecules in space for energy transfer.[1,2] Self-assembly processes, in which individual components associate spontaneously in a predetermined fashion, have emerged as one of the most powerful "bottom-up" techniques to mimic such orderliness for the preparation of well-organized optoelectronic materials.[3] However, a suitable structural matrix that allows both orientation and proximity between donor and acceptor units is required to obtain the appropriate spatial organization for efficient energy transfer. Indeed, without such an arrangement, fine control of energy transfer is not possible. Porous materials built of a solid-state array of self-assembled peptide nanotubes (SPNs), for which the homo- and/or heterodimerization can be easily controlled, would be of great interest.[4] Self-assembly of biomolecules that are capable of selectively forming either homo- and/or heterodimeric entities represents one of the great challenges today because, in general, current procedures do not provide sufficient recognition power for the selective assembly in either homo- or heteromeric fashion.[5] In nature, protein-subunit interactions (either homodimer or heterodimer) are an important phenomena in regulation and catalysis and appear to constitute an economical means of achieving structural diversity and functional versatility.[6] One would expect that the same goals may be achieved by the development of synthetic assemblers that are capable of selectively forming homo- and/or heterodimeric species. Herein, we report the controlled fabrication of homo- and heterodi meric light-harvesting nanobiomaterials through the self-organization of cyclic peptides (CPs). These systems can act as platforms for efficient energy transfer by providing an op timized spatial distribution.

As part of an extensive program directed towards the design, synthesis, and structural and functional evaluation of

[a] R. J. Brea, M. J. Pérez-Alvite, M. Panciera, Prof. Dr. L. Castedo, Prof. Dr. J. R. Granja
Departamento de Química Orgánica y
Unidad Asociada al C.S.I.C. Centro Singular de
Investigación en Química Biológica y Materiales Moleculares
Campus Vida
Universidad de Santiago
15782 Santiago de Compostela (Spain)
Fax: (+34) 981-595012
E-mail: juanr.granja@usc.es

[b] Prof. Dr. M. Mosquera
Departamento de Química Física y
Centro Singular de Investigación en
Química Biológica y Materiales Moleculares
Campus Vida
Universidad de Santiago
15782 Santiago de Compostela (Spain)

The Supporting Information for this article contains Figures SI-1–12, the ^{1}H and ^{13}C NMR, NOESY and/or ROESY, and FTIR spectra of peptides **9**, **10a**, **10b**, **10c**, **11a**, **11b**, **11c**, **12a**, **12c**, **12d**, and **12f**, together with the ^{1}H NMR spectra of compounds **13** and **14**, the ^{1}H NMR, NOESY, and/or ROESY spectra of heterodimers $\mathbf{D_{9a/10a}}$ and $\mathbf{D_{11a/12a}}$, and the UV spectra of peptides **11c**, **12c**, and **12f** and is available on the WWW under http://dx.doi.org/10.1002/asia.201000545.

peptide nanotubes,[4] we recently developed a novel class of CPs in which α-amino acids are alternated with cyclic γ-amino acids [such as γ-Ach (3-aminocyclohexanecarboxylic acid, Scheme 1, **1**–**3**) or γ-Acp (3-aminocyclopentanecarboxylic acid, Scheme 1, **4**–**8**)], to give systems with large homodimerization association constants.[7–9] Of particular interest is the preferential heterodimer formation between γ-Ach-based and γ-Acp-based cyclic α,γ-hexapeptides, in which the selective formation of the heterodimer is driven by backbone-to-backbone hydrogen-bonding interactions.[10–12] This is a very opportune property, because it allows side chain modifications to be exploited for other purposes without affecting the self-assembly properties, as exemplified by our recent findings on electron and/or energetic transfer processes.[13] Herein, we report a further extension of the selective heterodimer formation between cyclic α,γ-octapeptides based on γ-Ach residues with those containing γ-Acp. In these systems the preferential heterodimer formation is, once again, driven by the backbone–backbone interactions, as well as by the entropy of mixing (ΔS_{mix}).[11,14] Although the ΔS_{mix} is expected to increase, the heterodimer formation should not alter significantly the overall trend in association constants.

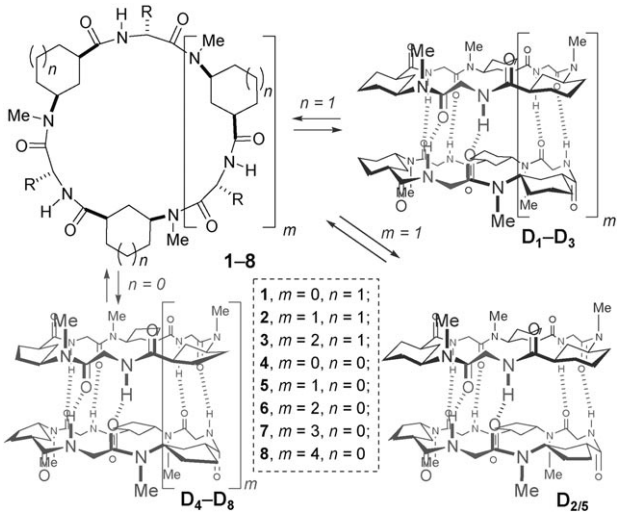

Scheme 1. α,γ-Cyclopeptides (**1**–**8**) and their corresponding dimer models ($\mathbf{D_1}$–$\mathbf{D_8}$). For clarity, amino acid side chains have been omitted from the representations of the nanotube and dimers.

Abstract in Spanish: Los ciclooctapéptidos compuestos de α-aminoácidos alternados con γ-aminoácidos cíclicos (ácidos *cis*-3-aminocicloalcanocarboxílicos) dan lugar a dímeros cilíndricos mediante un proceso de autoensamblaje molecular mediante la formación de una hoja plegada β. La formación de los heterodímeros es más favorable que la formación de los correspondientes homodímeros y esta discriminación se debe a las interacciones entre los esqueletos peptídicos y no al tipo de α-aminoácido que componen los cíclopéptide. Esto permite la preparación de una red de equilibrios de autoensablaje molecular entre distintos componentes ciclopetídicos marcados con fluoróforos que se han utilizado en el diseño de complejos de captura y conversión de luz mediante la adecuada disposición de las unidades dadoras y aceptoras que podría tener utilidad en el diseño de fotosistemas artificiales eficientes.

Results and Discussion

Cyclic octapeptides *cyclo*[(D-Leu-L-^{Me}N-γ-Acp)$_4$-] (**9**),[7b] *cyclo*[(D-Phe-L-^{Me}N-γ-Ach)$_4$-] (**10a**),[7c] and *cyclo*[(D-Ser(Bn)-L-^{Me}N-γ-Ach)$_4$-] (**10b**) were synthesized first (Scheme 2). The ^{1}H NMR spectra of these compounds in nonpolar solvents reflect the typical features of homodimer formation ($\mathbf{D_9}$, $\mathbf{D_{10a}}$, and $\mathbf{D_{10b}}$, respectively), for example, coupling constants ($J_{NH,H\alpha}$ = 9.5, 8.6, and 8.4 Hz for **9**, **10a**, and **10b**, respectively) and the downfield shift of the NH signal of α-Aa (δ = 8.33, 8.57, and 8.41 ppm for **9**, **10a**, and **10b**, respectively). The FTIR spectra in chloroform show the characteristic bands of β-sheet-like hydrogen bonding.[7,15] In all of these samples, the association constant for homodimer formation must be greater than $10^5\,M^{-1}$, based on the fact that the location of the N–H signals remains constant at concentrations as low as 1×10^{-4} M, regardless of whether the solvent contained 30% methanol or the samples were heated at 323 K.

The possibility of heterodimer formation was followed and confirmed by the successive additions of **10a** (from zero to 1.7 equivalents) to a chloroform solution of **9** (1.7 mM). This experiment resulted in the emergence of a new set of signals in the ^{1}H NMR spectrum that did not correspond to either of the possible homodimers (Figure 1 and Figure SI-1 in the Supporting Information). The dimeric nature of the new species, $\mathbf{D_{9/10a}}$, was confirmed by nuclear Overhauser effect (nOe) cross-peaks between the signals of Hγ_{Acp} (δ = 4.96 ppm) and Hα_{Ach} (δ = 2.67 ppm), and also Hγ_{Ach} (δ = 4.33 ppm) and Hα_{Acp} (δ = 3.17 ppm).

To determine the interactions (backbone versus side-chain interactions) responsible for the preferential formation of heterodimeric assemblies, *cyclo*{[D-Ser(Bn)-L-^{Me}N-γ-Ach]$_4$-} (**10b**) was added to CP **9** to study the formation of the corresponding heterodimer $\mathbf{D_{9/10b}}$ (Scheme 2). Any significant change in the heterodimer formation with respect to previous experiments could be attributed to the differences between the side-chain cross-strand interactions. Analysis of the ^{1}H NMR spectrum of the 1:1 mixture of the two peptides in chloroform again reveals the preferential formation of heterodimer $\mathbf{D_{9/10b}}$ (see Figure SI-2 in the Supporting Information). This result suggests that the selective formation of the heterodimer is mainly driven by the backbone–backbone hydrogen-bonding interactions between the Acp- and the Ach-containing CPs in which the better complementarity between the donors and acceptors of the two CPs induces the preferred formation of the heterodimeric form.[10,14]

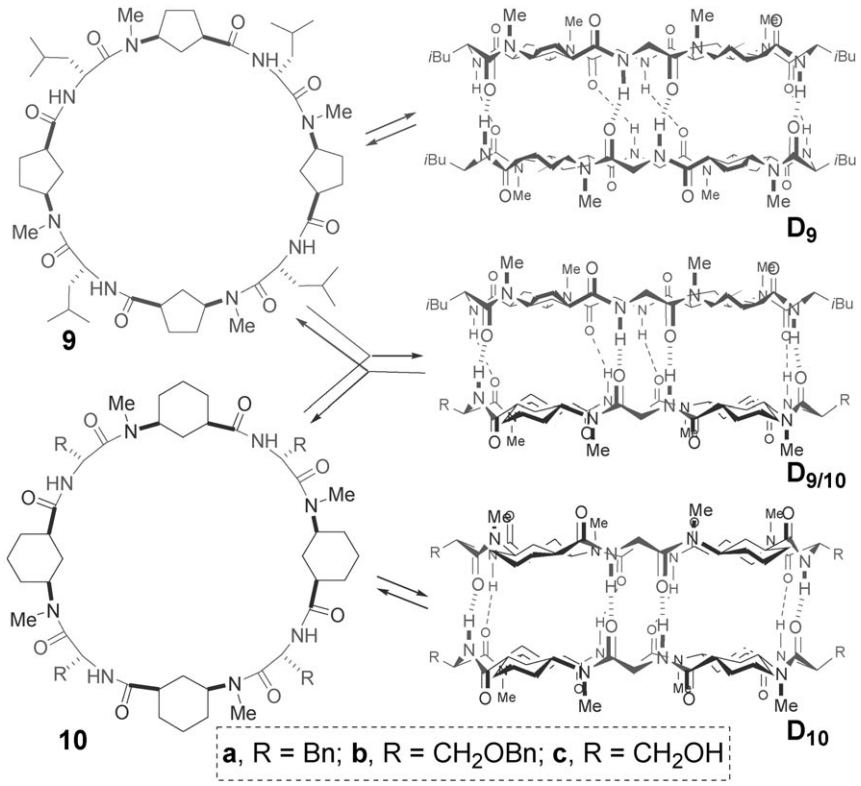

Scheme 2. Structures of Acp-based (**9**) and Ach-based (**10a–c**) fourfold symmetric cyclic octapeptides and their corresponding homodimers ($\mathbf{D_9}$ and $\mathbf{D_{10a-c}}$) and heterodimers ($\mathbf{D_{9/10a}}$, $\mathbf{D_{9/10b}}$ and $\mathbf{D_{9/10c}}$).

A new peptide, *cyclo*[(D-Ser-L-^{Me}N-γ-Ach)$_4$-] (**10c**), obtained by hydrogenation of **10b** (10% Pd/C, balloon pressure), was prepared with the aim of evaluating whether the potential side-chain/side-chain interactions between serine hydroxy groups in its homodimer form ($\mathbf{D_{10c}}$) play an important role in stabilizing the system or if formation of the heterodimer is still more favorable.[16] Although CP **10c** is not very soluble in nonpolar solvents, analysis of its ^{1}H NMR spectrum in chloroform again reveals the formation of the corresponding homodimer $\mathbf{D_{10c}}$ with a large association constant. Addition of one equivalent of a solution of **10c** (8.4 mM) in methanol to a chloroform solution of **9** (1.7 mM) resulted, once again, in the predominant formation of the heterodimeric species ($\mathbf{D_{9/10c}}$) (Figure SI-3 in the Supporting Information) confirming the predominant effect of backbone–backbone interactions over side chain-side chain interactions.

To investigate whether self-assembly might be significantly affected by interactions between amino acid side chains on adjacent CPs in more complex systems, new octapeptides *cyclo*{[D-Phe-L-^{Me}N-γ-Ach-D-Ser(Bn)-L-^{Me}N-γ-Ach]$_2$-} (**11a**), *cyclo*{[D-Phe-L-^{Me}N-γ-Acp-D-Ser(Bn)-L-^{Me}N-γ-Acp]$_2$-} (**12a**), and *cyclo*{[D-Phe-L-^{Me}N-γ-Acp-D-Glu(Bn)-L-^{Me}N-γ-Acp]$_2$-} (**12d**) were synthesized (Scheme 3). These CPs all present twofold symmetry instead of the fourfold symmetry of previously described CPs (**9** and **10a–c**). For this reason, these systems can form two non-equivalent homodimers that differ in the cross-strand interactions between monomers; i) the eclipsed homodimer, in which identical amino acids face each other (such as Phe to Phe, Ser to Ser, or Glu to Glu) and ii) the alternated dimer in which Phe faces the other amino acids (Ser for **12a** or **12b**, and Glu for **12d** and **12e**).[17] In addition, the functional group of Ser and Glu

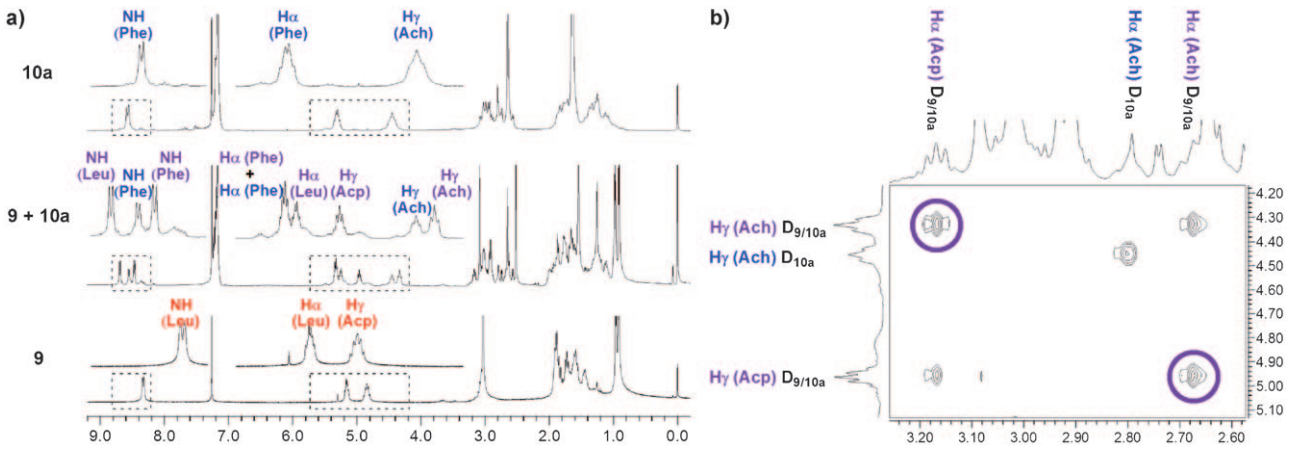

Figure 1. a) ^{1}H NMR spectra corresponding to the formation of heterodimer $\mathbf{D_{9/10a}}$ by addition of 1.7 equivalents of **10a** to a 1.7 mM $CDCl_3$ solution of **9** (298 K). Signals in purple correspond to the heterodimer $\mathbf{D_{9/10a}}$. b) ROESY spectrum (C_αH and C_γH of the γ-amino acids) of a 1:1.7 mixture of CPs **9** and **10a**, showing $H\gamma_{Acp}$(**9**)-$H\alpha_{Ach}$(**10a**) and $H\alpha_{Acp}$(**9**)-$H\gamma_{Ach}$(**10a**) nOe cross-peaks in heterodimer $\mathbf{D_{9/10a}}$.

CHEMISTRY
AN ASIAN JOURNAL

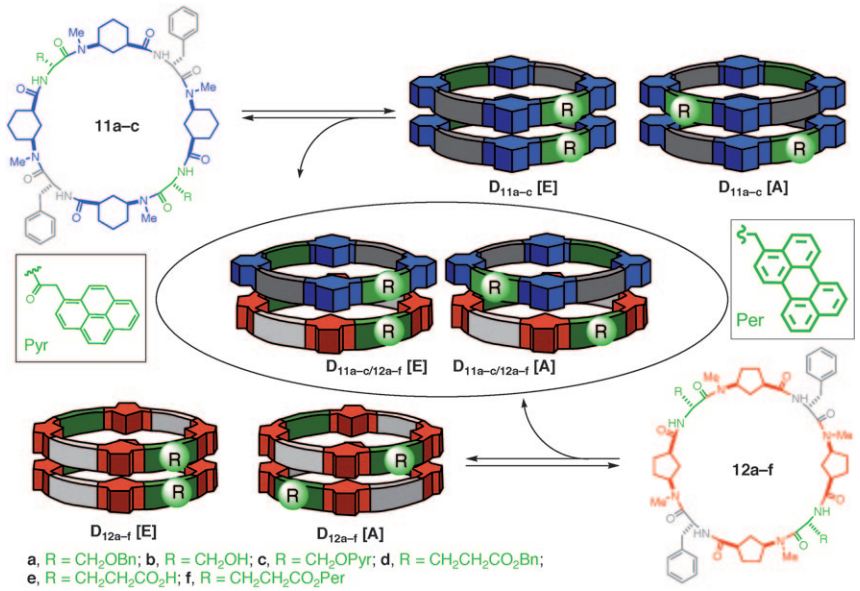

Scheme 3. Structures of Ach-based (**11a–c**) and Acp-based (**12a–f**) twofold symmetric cyclic octapeptides and models of their corresponding two non-equivalent (eclipsed **[E]** and alternated **[A]**) homodimers ($\mathbf{D}_{11a-c}$ and $\mathbf{D}_{12a-f}$) and heterodimers ($\mathbf{D}_{11a-c/12a-f}$).

side chains can be used to introduce additional groups for studying other properties. As expected, the ^{1}H NMR spectra of these CPs in chloroform showed two sets of signals that correspond to the two dimers both of which reflect β-sheet-like hydrogen bonding between monomers in the all-trans conformation. Only CP **11a** showed the preferential formation of one dimer (alternated) over the eclipsed one ($\mathbf{D}_{11a}$**[A]**/$\mathbf{D}_{12a}$**[E]**≈14:1), while the other two peptides (**12a** and **12d**) showed a similar ratio of both dimers (eclipsed, $\mathbf{D}_{12a}$**[E]** and $\mathbf{D}_{12d}$**[E]**, versus alternated, $\mathbf{D}_{12a}$**[A]** and $\mathbf{D}_{12d}$**[A]**; Table 1, entries 1, 4, and 7). The dimer ratios were not dependent on peptide concentration or temperature. In the case of Ach-based CP **11a**, the predominant formation of the alternated dimer ($\mathbf{D}_{11a}$**[A]**) was attributed to the rigidity derived from the cyclohexanecarboxylic acid and to the difference in the bulk of the side chains of Phe and Ser, which might slightly distort the flat conformation allowing the Ser residues to form stronger hydrogen bonds with Phe.[7c]

Table 1. Ratio between eclipsed and staggered dimers of Acp and Ach-based CPs.

Entry	Dimer	Subunit 1 [R]	Subunit 2 [R]	D[E]/ D[A][a]
1	$\mathbf{D}_{11a}$	**11a**, R = CH_2OBn	**11a**, R = CH_2OBn	1:14
2	$\mathbf{D}_{11b}$	**11b**, R = CH_2OH	**11b**, R = CH_2OH	1:6
3	$\mathbf{D}_{11c}$	**11c**, R = CH_2OPyr	**11c**, R = CH_2OPyr	1:10
4	$\mathbf{D}_{12a}$	**12a**, R = CH_2OBn	**12a**, R = CH_2OBn	1:1
5	$\mathbf{D}_{12b}$	**12b**, R = CH_2OH	**12b**, R = CH_2OBn	1:1
6	$\mathbf{D}_{12c}$	**12c**, R = CH_2OPyr	**12c**, R = CH_2OPyr	1:1
7	$\mathbf{D}_{12d}$	**12d**, R = $(CH_2)_2CO_2Bn$	**12d**, R = $(CH_2)_2CO_2Bn$	1:1.2
8	$\mathbf{D}_{12e}$	**12e**, R = $(CH_2)_2CO_2H$	**12e**, R = $(CH_2)_2CO_2H$	1:1.2
9	$\mathbf{D}_{12f}$	**12f**, R = $(CH_2)_2CO_2Per$	**12f**, R = $(CH_2)_2CO_2Per$	1:0.6
10	$\mathbf{D}_{11a/12a}$	**11a**, R = CH_2OBn	**12a**, R = CH_2OBn	1:1

[a] Ratio determined by using ^{1}H NMR spectroscopy.

The preferential formation of the corresponding heterodimers was confirmed by the addition of **11a** to a solution of **12a** (2.8 mM) in chloroform, which once again resulted in the appearance of a new set of signals in the ^{1}H NMR spectrum that did not correspond to either of the possible homodimers (Figure SI-4 in the Supporting Information). Interestingly, the ratio between the eclipsed and alternated heterodimeric assemblies ($\mathbf{D}_{11a/12a}$**[E]** and $\mathbf{D}_{11a/12a}$**[A]**) was 1:1 (Table 1, entry 10). This finding again corroborated that the selective formation of the heterodimeric ensembles is driven mainly by the β-sheet hydrogen bonding interactions and is independent of the side-chains of the α-Aa employed in the CPs. In addition, the flexibility of the cyclopentyl rings allows the Acp-based CPs, such as **12a**, to fit their conformation to the buckled form of the Ach-based CP regardless of the cross-strand interaction.

Steady-State and Time-Resolved Fluorescence Studies

Fluorescence methods have been extensively used in the study of self-assembly processes in supramolecular chemistry,[18] but their application to the study of SPNs is still recent.[13,19] We proceeded to use the spectral properties of pyrene (i.e., excimer emission) to evaluate different systems involving homo- and heterodimeric entities in equilibrium. The information derived from the CPs containing pyrene moieties was completed by using a second chromophore such as perylene, which could act as a donor for fluorescence resonance energy transfer (FRET, Figure 2b). Perylene was chosen because it has spectroscopic characteristics such as high quantum yield and spectral absorption overlap with the emission spectrum of pyrene, thus making these two moieties an efficient FRET pair for studying heterodimeric systems.[20] In addition perylene can also form excimer species that could be used in evaluating homodimer properties. Pyrene and perylene excimers formation and FRET effects can be combined to analyze complex intermolecular association systems.

The fluorescence network developed in our study was formed by different equilibria involving three fluorescently labeled α,γ-CPs (Scheme 3): *cyclo*{[D-Phe-L-^{Me}N-γ-Ach-D-

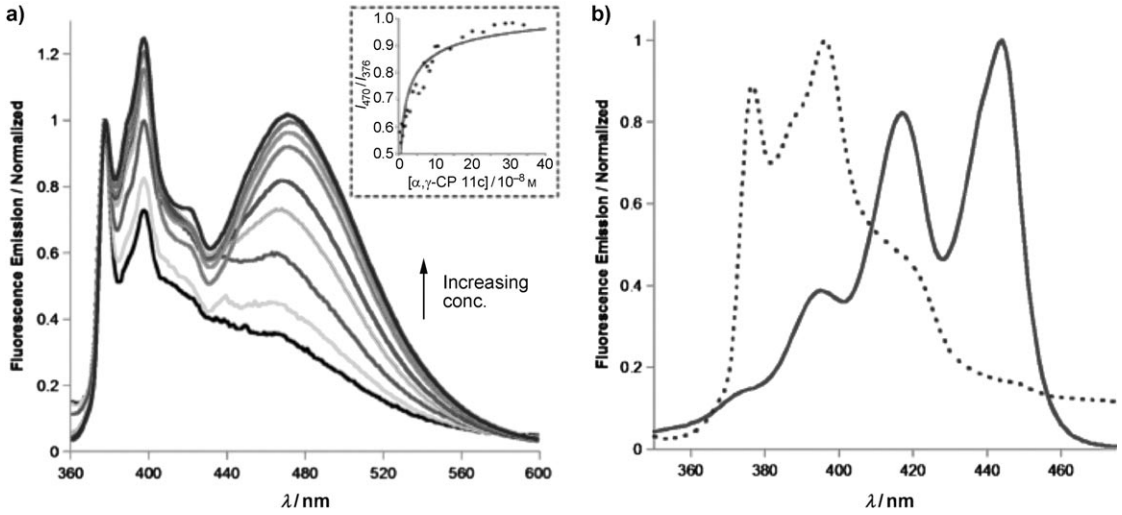

Figure 2. a) Pyrene fluorescence emission of **12c** ($\lambda = 340$ nm excitation wavelength) in $CHCl_3$ from 3.35 nM to 0.23 μM, denoting homodimer formation. Inset shows the titration data for K_A calculation. b) Absorption spectrum of perylene (solid line) showing the overlap with pyrene emission (dashed line). All spectra were normalized for the sake of comparison.

Ser(Pyr)-L-^{Me}N-γ-Ach]$_2$-} (**11c**), *cyclo*{[D-Phe-L-^{Me}N-γ-Acp-D-Ser(Pyr)-L-^{Me}N-γ-Acp]$_2$-} (**12c**), and *cyclo*{[D-Phe-L-^{Me}N-γ-Acp-D-Glu(Per)-L-^{Me}N-γ-Acp]$_2$-} (**12f**). All of these Acp-based and Ach-based CPs were synthesized as follows. Previously obtained peptides **11a**, **12a**, and **12d** were deprotected (H_2, Pd/C, or HBr/TFA) to provide the corresponding CPs **11b**, **12b**, and **12e**, respectively. The unprotected Acp-based CPs showed almost the same ratio between the isomeric dimers as the protected ones (1:1 for **12b** and 1:1.2 for **12e**; Table 1, entries 5 and 8), whereas unprotected Ach-based CP **11b** showed a slight increase in the eclipsed/alternated ratio (from 1:14 for **11a** to 1:6 for **11b**; Table 1, entries 1 and 2). Peptides **11b** and **12b** were subsequently coupled with 1-pyreneacetic acid in the presence of *N*,*N*′-di isopropylcarbodiimide/4-(dimethylamino)pyridine (DIC/DMAP) to give **11c** and **12c**, respectively, whereas CP **12f** was prepared by analogous coupling of **12e** with perylen-3-ylmethanol (**14**).[21] The NMR spectra of the resulting peptides in chloroform exhibited clear β-sheet signals, characteristic of homodimeric structures, in which the two non-equivalent dimers are slowly exchanging on the NMR timescale. As expected for **12c**, the ratio between eclipsed and alternated forms did not change with the introduction of a pyreneacetyl group into the serine side-chain (1:1 for $\mathbf{D_{12c}[E]/D_{12c}[A]}$; Table 1, entry 6). However, fluorescent Ach-based CP **11c** presented a different ratio between non-equivalent dimers ($\mathbf{D_{11c}[E]/D_{11c}[A]}$) than the corresponding unprotected CP (**11b**), with an increase observed in the proportion of the alternated dimer (1:10; Table 1, entry 6). This is close to the ratio observed for the benzyl ester **11a** and suggests that perhaps the observed stabilization of the eclipsed form of the CP containing the free hydroxy group (**11b**) could arise from the formation of week hydrogen-bonding interactions between the side chains of the serine residues. Surprisingly, the introduction of the perylene moiety into CP **12e** led to the inversion of the ratio between eclipsed and alternated assemblies (from 1:1.2 for $\mathbf{D_{12d}[E]/D_{12d}[A]}$ or $\mathbf{D_{12e}[E]/D_{12e}[A]}$ to 1:0.6 for $\mathbf{D_{12f}[E]/D_{12f}[A]}$; Table 1, entry 9), with the eclipsed dimer now the main form. Preferential formation of the eclipsed dimer ($\mathbf{D_{12f}[E]}$) instead of the alternated one ($\mathbf{D_{12f}[A]}$) can perhaps be attributed to an edge-face interaction between perylene moieties, vide infra.

The emission of CPs containing pyrene moieties presents two characteristic well-defined emission bands. The pyrene band, in the ultraviolet region, is identified by its typical vibronic structure, and the emission at longer wavelength corresponds to the short-lived dimeric species—one member of which is in an electronically excited state, called an excimer.[22] The relative intensities of the two bands reflect the ratio between monomer and dimer in solution. The first equilibrium studied was the homodimerization process of the Acp-based cyclic octapeptide **12c** because in nonpolar solvents the dimers formed ($\mathbf{D_{12c}[E]}$ and $\mathbf{D_{12c}[A]}$, Scheme 3) exist in an almost equimolecular ratio. Dilute solutions of **12c** (0.15 nM in chloroform) showed only the characteristic emission spectrum of the pyrene moiety, with two maxima at $\lambda = 377$ and 397 nm. Addition of successive aliquots of a concentrated stock solution of this CP (1.5 μM) resulted in the appearance of the excimer-emission band at $\lambda = 470$ nm (Figure 2a).[23] Considering that the formation of excimers is geometrically only possible in the eclipsed dimer ($\mathbf{D_{12c}[E]}$), we used the observed excimer band to calculate its homodimerization binding constant, with a value of K_A ($CHCl_3$) = $7.3 \times 10^8\ M^{-1}$ obtained (Figure 2a, inset).[24] In this way, the formation of two additional hydrogen-bonding interactions, in comparison to cyclic hexapeptides,[13b] leads to an increase in the association constant by almost three orders of magnitude. This is by far the largest association constant measured for a nanotube-forming CP and is five orders of magnitude higher than that of the dimer-forming CPs made of alternating D- and L-α-amino acids (α-D,L-CP), which has an identical number of hydrogen-bonding interactions.[25] Analogous

results were obtained in a 20% DMSO/$CHCl_3$ solution, although, as expected, the association constant is slightly lower, K_A (1:4 DMSO/$CHCl_3$) $= 1.5 \times 10^7\,M^{-1}$ (Figure SI-5 in the Supporting Information). Further experiments were carried out in polar media (CH_3CN) and the characteristic excimer band was observed.[26] This band disappeared on addition of different aliquots of a more strongly hydrogen bonding competing solvent such as milliQ water (Figure SI-6 in the Supporting Information).[27]

The second equilibrium analyzed was the homodimerization process of CP **11c** (Scheme 3). As described above, at low concentration (0.12 μM) in $CHCl_3$ this CP showed the typical emission spectrum of the pyrene moiety. Successive addition of aliquots of a concentrated stock solution of **11c** (12.0 μM) resulted in the appearance of the corresponding pyrene excimer. In this case, as mentioned before, the excimer formation is only geometrically possible for the minor dimer (**D_{11c}[E]**), a situation that made the measurement of its association constant more difficult and less accurate. Despite this, the association constant was estimated to be of a similar order, albeit slightly lower, than that for the Acp-based CPs, K_A ($CHCl_3$) $= 1.2 \times 10^8\,M^{-1}$ (Figure SI-7 in the Supporting Information), as predicted by our previous DFT calculations.[11]

Addition of Ach-based CP **11a** to a 0.13 μM chloroform solution of homodimer **D_{12c}** resulted in an increase in the natural emission of pyrene at $\lambda = 377$ and 397 nm, and a reduction in the $\lambda = 472$ nm pyrene excimer band (Figure SI-8 in the Supporting Information). This observation is consistent with the formation of heterodimer **$D_{11a/12c}$** as homodimer **D_{12c}** disappears.[28] As expected, addition of one equivalent of **12a**, which does not have a fluorophore in its side chain, to a solution of Ach-based CP **11c** resulted in the disappearance of the pyrene excimer-emission band, again consistent with formation of the heterodimeric species **$D_{11a/12c}$** and the disruption of excimer-forming homodimer **D_{12c}**. Both results clearly indicate that the homodimeric model is responsible for the excimer emission and that heterodimer assemblies are more stable than the corresponding homodimers.

Preferential heterodimer formation was also studied through FRET processes between pyrene and perylene moieties of corresponding CPs (**11c** and **12f**, respectively).[29] Irradiation at $\lambda = 340$ nm of an 8.0 μM chloroform solution of perylene-derivatized CP **12f** resulted in a small emission characterized by the three feature bands (at $\lambda = 449$, 479, and 513 nm) of the perylene system. Addition of successive aliquots of complementary CP (**11c**) led to a clear increase in the fluorescence emission intensity of the three bands (Figure 3b), which must arise from intramolecular FRET between pyrene and perylene in the resulting heterodimeric complex **$D_{11c/12f}$**.[20,30] As expected, inverse titration by the addition of successive aliquots of **12f** to a 6.0 μM solution of **11c** again led to a substantial increase in the fluorescence emission intensity of the perylene bands and a significant reduction of the pyrene emission, denoting once more the heterodimeric FRET process (Figure SI-9 in the Supporting Information). As previously indicated, the efficient energy transfer is possible, owing to the spectral overlap between the two fluorophores (Figure 3b).

Disruption of the supramolecular heterodimeric species **$D_{11c/12f}$** was achieved by addition of competitive CP **11a**, resulting in a reduction of the three signals of perylene and an increase in the typical emission of pyrene (Figure SI-10 in the Supporting Information). This result is a consequence of the formation of the heterodimers **$D_{11a/12f}$** and **$D_{11a/11c}$**, which do not have any energy transfer process.

These results demanded a full characterization of the dynamic processes taking place using time-resolved fluorescence techniques. Irradiation of homodimer **D_{12c}** resulted in

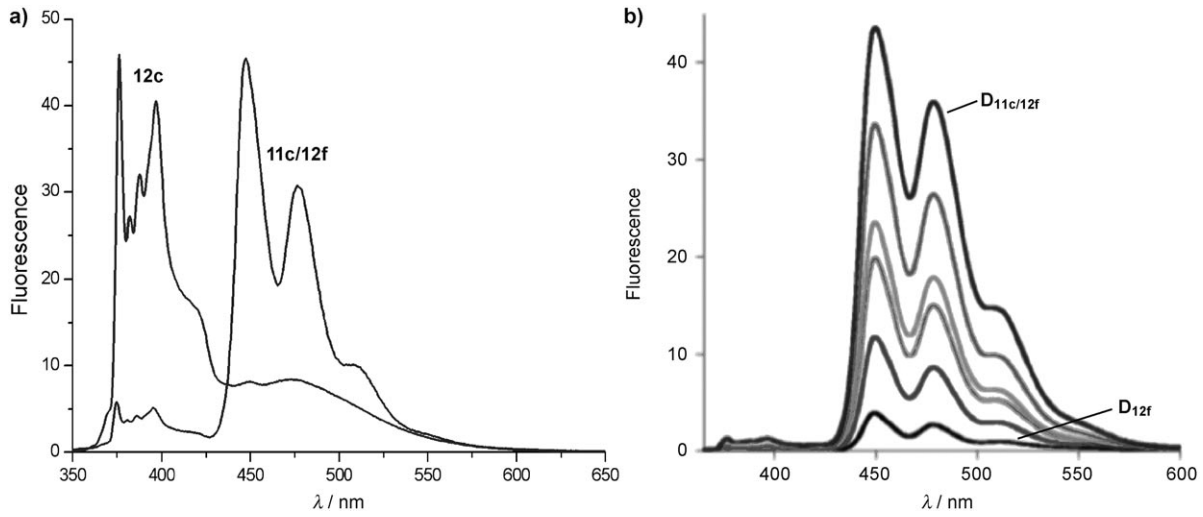

Figure 3. a) Fluorescence emission of **12c** (5×10^{-6} M), excitation at $\lambda = 345$ nm. Fluorescence emission of a mixture of **11c** (5×10^{-6} M) and **12f** (5×10^{-6} M), excitation at $\lambda = 345$ nm. b) Fluorescence emission of homodimer **D_{12f}** and heterodimer **$D_{11c/12f}$**. Addition of successive aliquots of **11c** (from 0 to 1.2 eq) to a 8.0 μM solution of **12f** increases the fluorescence emission intensity of perylene bands, denoting an efficient Per/Pyr FRET process in the resulting heterodimeric **$D_{11c/12f}$** complex.

a fluorescence decay that could be fitted to a three exponential model with three different times of 25, 6.4, and 0.3 ns (Figure 4). The longer time (25 ns), with a contribution of 95%, corresponds to the normal pyrene emission decay in a non-deoxygenated solvent and it must correspond to the dimer ($\mathbf{D_{12c}[A]}$) for which excimer formation is geometrically impossible (Scheme 3). The shorter lifetime of 6.4 ns, with a 5% contribution, and the 0.3 ns time, with a residual contribution of only 0.2%, are assigned to the process of conformational change that gives the required geometrical arrangement for excimer formation—that is, the dimer with pyrene side chains in register ($\mathbf{D_{12c}[E]}$, Figure 4c). Fluorescence decay measurements at the excimer emission wavelength ($\lambda = 480$ nm) also showed a three exponential decay (22.7, 7.4, and 2.1 ns). The two shortest lifetimes are associated with negative pre-exponential factors, whereas the long lifetime has a positive pre-exponential factor for which the numerical value is somewhat higher than the absolute value of the sum of the previous two. The 22.7 ns time corresponds to the excimer decay that, as can be deduced from the pre-exponential factors, is mainly formed in the excited state. This means that in the ground state, the two pyrene moieties must not be interacting with each other to any great extent. From the pre-exponential factors it can be inferred that at least 70% of the excimer-emitting moieties are formed in the excited state. This conformation can come from two different conformers that evolve to the excimer formation. The dimer equilibrium between alternated and eclipsed forms is slower, with both species observed in the NMR spectrum; as this equilibrium is slower than the NMR time scale, we conclude that this change in conformation is related with the side chain that links pyrene and the CP backbone. These two conformers are in a 7:1 ratio and the most abundant is the one that evolves in 7.4 ns.

The time-resolved emission of CP **12f** resulted in a fluorescence decay that could be fitted again to a three exponential process, for which the longest lifetime was 4 ns, which corresponds well with the typical perylene emission, with an 80% contribution (Figure SI-11 in the Supporting Information).[31] The other two exponential factors of 1.4 and 0.2 ns have a contribution of 18 and 2%, respectively. This could represent the existence of conformers that evolve towards an excimer, although this could not be confirmed because the perylene excimer could not be observed under these conditions.[29]

The emission temporal dependence of the heterodimeric complex $\mathbf{D_{11c/12f}}$ at the perylene band ($\lambda = 480$ nm), as the pyrene is excited ($\lambda = 333$ nm), can again be fitted to a three

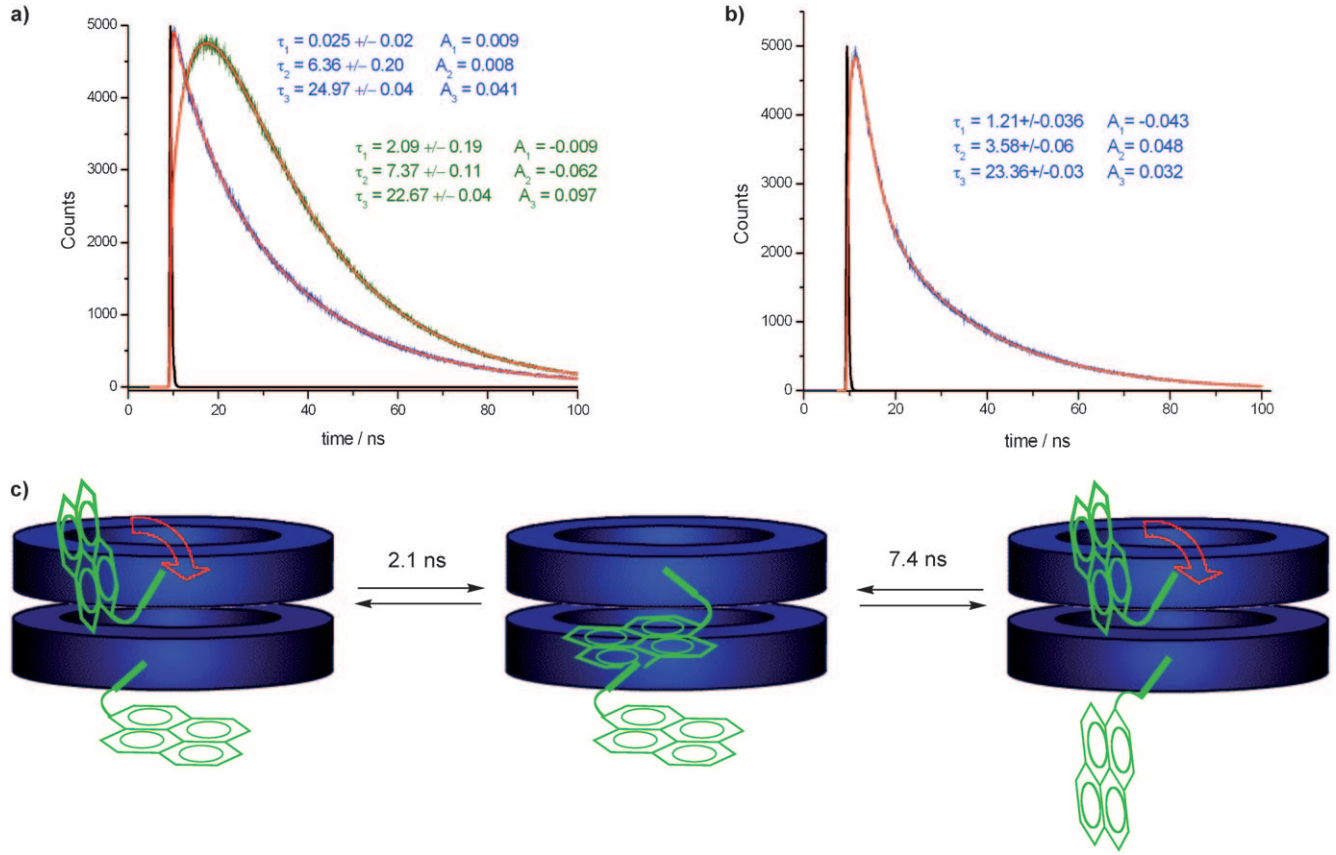

Figure 4. a) Time resolved $\lambda = 395$ nm emission (blue) of 5 μM monomeric CP **12c**, with excitation at $\lambda = 333$ nm; $\lambda = 450$ nm emission (green) of homodimeric $\mathbf{D_{12c}}$. b) Time resolved $\lambda = 480$ nm emission of heterodimeric $\mathbf{D_{11c/12f}}$ (5 μM **11c** and 3 μM **12f**) with excitation at $\lambda = 333$ nm. The black line represents the laser pulse and the Red lines are the best fit to the experimental data. c) Proposed conformational change of eclipsed dimer to form the excimer upon pyrene excitation.

exponential process for which the two shortest time exponentials, 1.2 and 3.6 ns,[31] have the same amplitude, but opposite sign (Figure 4b). Consequently, the emitting species with a lifetime of 3.6 ns comes from the one with the shortest lifetime (1.2 ns). The emission time of perylene is 3.6 ns and this results from the energy transfer from the pyrene. The 1.2 ns lifetime was assigned to the energy-transfer process. The transfer-energy constant is $(1/1.2)=0.8\ ns^{-1}$, which represents the weighted-average value of the different conformations and distances between the donor (pyrene) and the acceptor (perylene) moieties. The third time, 23.4 ns, corresponds to the pyrene emission from the excimer-forming homodimer ($\mathbf{D_{11c}}$), which in this case is in excess. The lifetime of the energy transfer process (1.2 ns), together with the previously estimated Förster radius (R_0) of 22 Å,[20b,e] allowed us to determine an average pyrene–perylene distance of 18 Å, with 96% efficiency in the transfer process by using Equation (1):

$$r = \frac{R_0}{(\tau_D^0/\kappa_t)^{1/6}} \quad (1)$$

For which τ_D^0 is the excited-state lifetime of pyrene in the absence of transfer (25 ns) and κ_t is the transfer-energy constant ($0.8\ ns^{-1}$).[32] This distance corresponds to the dimers in which pyrene and perylene are not in proximity ($\mathbf{D_{11c/12f}[A]}$). The other form ($\mathbf{D_{11c/12f}[E]}$), in which both fluorophores are in close contact, must have an even faster transfer that is not detectable in the nanosecond timescale.

Time-resolved fluorescence experiments at the perylene band ($\lambda=450$ nm) when the pyrene is excited ($\lambda=333$ nm) of heterodimer $\mathbf{D_{11c/12f}}$ solutions, in which perylene-containing CP (**12f**) was in excess, gave similar results (see Figure 12-SI in the Supporting Information). The fluorescence decay could be fitted again to a three exponential process, for which the lifetime of 4.5 ns is the emission time of perylene, which is formed by the energy transfer from the pyrene, but also directly by the $\lambda=333$ nm light, because it is in excess compared to pyrene CP. This is the explanation for why, in this case, the 1.2 and 4.5 ns have the same amplitude, but opposite signs, as there is more excited perylene than pyrene. Finally, the third lifetime (14 ns) corresponds to the pyrene emission and derives from the small amount of monomer-emitting pyrenes.

Conclusions

In summary, analysis by using NMR and fluorescence spectroscopies have provided conclusive evidence that cyclic α,γ-octapeptide heterodimers of α,γ(Acp)-CPs with α,γ(Ach)-CPs, which are held together by β-sheet-like hydrogen bonds, are more stable than the corresponding homodimers. Pyrene-labeled CPs allowed measurement of the association constant and showed the strength of the β-sheet interaction responsible for homodimer formation; this interaction is stronger than those previously reported for CPs that form nanotubes, with the Acp-based dimers strongest ($>10^8\ M^{-1}$). Despite the strength of the interactions, there is clear selectivity for the heterodimer formation between Acp-based CPs and Ach-based CPs. The selective formation of the heterodimeric ensembles is driven mainly by the backbone-to-backbone hydrogen bonding interactions and is not a result of interstrand side chain–side chain interactions. This homo/hetero equilibrium allows the selective formation of a wide collection of supramolecular assemblies with potential applications as sensors, catalysts, and electronic/optical devices. Introduction of pyrene and perylene functionalities was particularly relevant for the design and characterization of a novel multicomponent system based on fluorescently derivatized α,γ-CPs. These materials were specifically tailored for studying networks involving homo- and heterodimerization processes. Exhaustive fluorescence studies have shown that such CPs act as suitable platforms for efficient energy transfer by providing an optimized spatial distribution between fluorophores, a characteristic that could be successfully used for the development of efficient light-harvesting/light-converting ensembles.

Experimental Section

Synthesis of 3-Formylperylene (13)[21,33]

An ice-cooled suspension of perylene (1.00 g, 3.96 mmol) in 1,2-dichlorobenzene (60 mL) was treated with 1,1-dichloromethyl methyl ether (466 μL, 5.15 mmol) [CAUTION: CARCINOGEN] and $TiCl_4$ (1.0 M solution in CH_2Cl_2; 5.94 mL, 5.94 mmol). The resulting mixture was stirred at 0 °C for 1 h, allowed to warm to room temperature, and poured onto ice (200 g) and HCl (conc. 10 mL). The organic layer was diluted with $CHCl_3$ (200 mL), washed with HCl (5%) (200 mL) and H_2O (3× 200 mL), dried over Na_2SO_4, and evaporated to dryness. The residue was purified by flash chromatography (100% $CHCl_3$) to give the desired compound 3-formylperylene as orange crystals [1.02 g, 92%, $R_f=0.74$ (100% $CHCl_3$)]. ^1H NMR ($CDCl_3$, 250.13 MHz): $\delta=10.25$ (s, 1H, CHO), 9.10 (d, $J=8.2$ Hz, 1H), 8.41–7.98 (m, 4H), 7.93–7.56 (m, 4H), 7.50 ppm (t, $J=7.8$ Hz, 2H); MS (ESI): *m/z* (%): 281 ($[M]H^+$, 100), 245 (78), 126 (72); HRMS (ESI): calcd for $C_{21}H_{13}O$ ($[M]H^+$): 281.0966; found: 281.0961.

Synthesis of Perylen-3-ylmethanol (14)[21]

A solution of 3-formylperylene (400.0 mg, 1.43 mmol) in a mixture of tetrahydrofuran/methanol (THF/MeOH, 2:1; 60 mL) was treated with sodium borohydride (56.7 mg, 1.50 mmol), and the mixture was stirred at RT for 30 min. The resulting mixture was diluted with H_2O (40 mL), acidified to pH 1–2 by addition of HCl (conc.), and finally extracted with $CHCl_3$ (2×200 mL). The combined organic layers were washed with H_2O (2×100 mL) and saturated aqueous $NaHCO_3$ (1×100 mL), dried over Na_2SO_4, and concentrated under reduced pressure. The crude material was purified by using flash chromatography (100% $CHCl_3$), to give perylen-3-ylmethanol [348 mg, 86%, $R_f=0.24$ (100% $CHCl_3$), yellow solid]. ^1H NMR ($CDCl_3$, 250.13 MHz): $\delta=8.30$–8.11 (m, 4H), 7.96 (d, $J=8.4$ Hz, 1H), 7.70 (d, $J=8.0$ Hz, 2H), 7.63–7.42 (m, 4H), 5.10 (s, 2H), 1.76 ppm (br s, 1H); MS (EI): *m/z* (%): 282 ($[M]^+$, 100), 265 (59), 252 (59); HRMS (EI): calcd for $C_{21}H_{14}O$ ($[M]^+$): 282.104465; found: 282.104829.

Peptide Synthesis

Linear peptides Boc-[(D-Leu-L-^{Me}N-γ-Acp)$_4$-]OFm, Boc-[(D-Phe-L-^{Me}N-γ-Ach)$_4$-]OFm, Boc-{[D-Ser(Bn)-L-^{Me}N-γ-Ach]$_4$-}OFm, Boc-{[L-Phe-D-^{Me}N-γ-Acp-L-Ser(Bn)-D-^{Me}N-γ-Acp]$_2$-}OFm, Boc-{[L-Phe-D-^{Me}N-γ-Ach-L-

Ser(Bn)-D-^{Me}N-γ-Ach]$_2$-}OFm, and Boc-{[L-Phe-D-^{Me}N-γ-Acp-L-Glu(Bn)-D-^{Me}N-γ-Acp]$_2$-}OFm were prepared following the synthetic strategy described previously.[10]

General Method for Amino Acid Coupling: Synthesis of Boc-[D-Leu-L-^{Me}N-γ-Acp-]OFm

A solution of **6b** (775 mg, 1.84 mmol) in 18 mL of trifluoroacetic acid/dichloromethane (TFA/DCM, 1:1) was stirred at RT for 15 min. The solvent was removed and the residue was dried under high vacuum for 3 h. The resulting TFA salt was dissolved in dry DCM (18 mL), after which D-Boc-Leu-OH·H_2O (467 mg, 2.02 mmol), 2-(1H-7-azabenzotriazol-1-yl)-1,1,3,3-tetramethyl uronium hexafluorophosphate methanaminium (HATU, 769 mg, 0.601 mmol), and *N,N*-diisopropylethylamine (DIEA, 1.29 mL, 7.36 mmol) were successively added. The mixture was stirred for 1 h at RT and the solution was poured into a separating funnel and washed with HCl (5%) and $NaHCO_3$ (sat.). The organic layers were dried over Na_2SO_4 and concentrated under reduced pressure to give a yellow oil, which was purified by flash chromatography (15–25% EtOAc/Hexanes) to give the target dipeptide as a white foam [897 mg, 91%, R_f=0.66 (50% EtOAc/hexanes)]. ^{1}H NMR ($CDCl_3$, 250.13 MHz): δ= 7.67 (d, J=7.3 Hz, 2H), 7.50 (d, J=7.3 Hz, 2H), 7.27 (td, J_1=7.4 Hz, J_2= 22.2 Hz, 4H), 5.24 (m, 1H), 4.85 (m, 1H), 4.70–4.30 (m, 3H), 4.12 (m, 1H), 2.76 (s, 3H), 2.64 (m, 1H), 2.08–1.05 (m, 18H), 0.88 ppm (ddd, J_1= 5.1 Hz, J_2=7.7 Hz, J_3=10.2 Hz, 6H); ^{13}C NMR ($CDCl_3$, 62.90 MHz): δ= 175.5 (CO), 173.2 (CO), 155.5 (CO), 143.5 (C), 141.2 (C), 127.7 (CH), 127.0 (CH), 124.7 (CH), 119.9 (CH), 79.3 (C), 65.8 (CH_2), 57.2 (CH), 53.9 (CH), 49.2 (CH), 46.9 (CH), 42.7 (CH_2), 41.5 (CH), 30.9 (CH_2), 29.0 (CH_3), 28.3 (CH_3), 27.5 (CH_2), 27.0 (CH_2), 23.4 (CH_3), 21.7 ppm (CH_3); MS (FAB$^+$): *m/z* (%): 535 ([*M*H]$^+$, 17), 479 (8), 435 ([*M*H−Boc]$^+$, 7); HRMS (FAB$^+$): calcd for $C_{32}H_{43}N_2O_5$ ([*M*H]$^+$): 535.31720; found: 535.31845.

General Method for Peptide Coupling

Synthesis of Boc-[(D-Leu-L-^{Me}N-γ-Acp)$_2$-]OFm: A solution of the dipeptide Boc-[D-Leu-L-^{Me}N-γ-Acp-]OFm (225 mg, 0.42 mmol) in 20% piperidine/DCM (5 mL) was stirred at RT for 20 min and the solvent was removed in vacuo. The residue was dissolved in DCM (10 mL), washed with HCl (5%), dried over Na_2SO_4, filtered, and concentrated to give Boc-[D-Leu-L-^{Me}N-γ-Acp-]OH, which was used without further purification.

A solution of Boc-[D-Leu-L-^{Me}N-γ-Acp-]OFm (225 mg, 0.42 mmol) in 4 mL of TFA/DCM (1:1) was stirred at RT for 15 min. The solvent was removed and the residue was dried under high vacuum for 3 h. The resulting dipeptide was dissolved in dry DCM (4 mL) to which Boc-[D-Leu-L-^{Me}N-γ-Acp-]OH, HBTU (176 mg, 0.46 mmol), and DIEA (294 μL, 1.68 mmol) were successively added. The mixture was stirred for 1 h at RT and the solution was washed with HCl (5%) and $NaHCO_3$ (sat.), dried over Na_2SO_4, and concentrated under reduced pressure. The residue was purified by flash chromatography (0–3% MeOH/CH_2Cl_2) to give Boc-[(D-Leu-L-^{Me}N-γ- Acp)$_2$-]OFm, as a white foam [270 mg, 83%, R_f=0.28 (3% MeOH in DCM)]. MS (FAB$^+$): *m/z* (%): 773 ([*M*H]$^+$, 100), 673 ([*M*H−Boc]$^+$, 14), 560 (22), 452 (48); HRMS: calcd for $C_{45}H_{65}N_4O_7$ ([*M*H]$^+$): 773.48533; found: 773.48575.

Synthesis of *cyclo*[(D-Leu-L-^{Me}N-γ-Acp)$_4$-] (9)[7b]: A solution of Boc-[(D-Leu-L-^{Me}N-γ-Acp)$_4$-]OFm (50.0 mg, 40.1 μmol) in 20% piperidine in DCM (400 μL) was stirred at RT for 20 min. The solvent was removed and the residue was dissolved in DCM (5 mL). The solution was washed with HCl (5%), dried over Na_2SO_4, filtered, and concentrated. The resulting residue was dissolved in 400 μL of TFA/DCM (1:1) and stirred at RT for 15 min. The solvent was removed and the residue was dried under high vacuum for 3 h and used without further purification. The linear peptide was dissolved in DCM (40.1 mL) and treated with TBTU (14.1 mg, 44.1 μmol), followed (dropwise) by DIEA (28 μL, 160.3 μmol) [an additional 1 equiv of TBTU (12.9 mg, 40.1 μmol), and 4 equiv of DIEA (28 μL, 160.3 μmol) were added when the starting material was observed by HPLC, and the resulting mixture was stirred for 3 h at RT to complete the reaction]. After 12 h, the solvent was removed under reduced pressure, and the crude mixture was purified by using HPLC to afford **9** as a white solid [29.0 mg, 76%, R_t=16 min (Phenomenex Maxsil-10 semipreparative column, 5–15% MeOH in CH_2Cl_2, 30 min)]. ^{1}H NMR ($CDCl_3$, 500.13 MHz): δ=8.33 (d, J=9.5 Hz, 1H, NH_{Leu}), 5.16 (m, 1H, Hα_{Leu}), 4.84 (m, 1H, Hγ_{Acp}), 3.06 (m, 1H, Hα_{Acp}), 3.03 (s, 3H, NCH_3), 2.09–1.14 (m, 9H, 3×CH_2 γ-Acp+CH_{2Leu}+CH_{Leu}), 0.94 ppm (dd, J_1=17.7 Hz, J_2=6.3 Hz, 6H, CH_{3Leu}); ^{13}C NMR ($CDCl_3$, 125.77 MHz): δ=174.9 (CO), 173.4 (CO), 54.6 (CH), 46.8 (CH), 43.3 (CH), 42.2 (CH_2), 32.8 (CH_2), 29.4 (NCH_3), 27.9 (CH_2), 26.9 (CH_2), 24.7 (CH), 23.4 (CH_3), 22.2 ppm (CH_3); FT-IR (293 K, $CHCl_3$): $\tilde{\nu}$=3309 (amide A), 3003, 2959, 1665, 1626 (amide I), 1536 cm^{-1} (amide II$_{II}$); MS (MALDI-TOF): *m/z* (%): 993 ([*M*+K]$^+$, 7), 975 ([*M*+Na]$^+$, 100), 953 ([*M*H]$^+$, 34); HRMS (MALDI-TOF): calcd for $C_{52}H_{88}N_8O_8Na$ ([*M*+Na]$^+$): 975.6617; found: 975.6573.

Synthesis of *cyclo*[(D-Phe-L-^{Me}N-γ-Ach)$_4$-] (10a)[7c]: Previously obtained from Boc-[(D-Phe-L-^{Me}N-γ-Ach)$_4$-]OFm (201 mg, 140 μmol) in the same way as **9** to yield, after HPLC purification, CP **10a** (112 mg, 70%); white solid. ^{1}H NMR ($CDCl_3$, 300.13 MHz): δ=8.57 (d, J=8.6 Hz, 1H, NH_{Phe}), 7.17 (m, 5H, Ar-H_{Phe}), 5.30 (dd, J=5.7 Hz, 1H, Hα_{Phe}), 4.45 (br s, 1H, Hγ_{Ach}), 3.00–2.71 (m, 3H, $CH_2\beta_{Phe}$+Hα_{Ach}), 2.64 (s, 3H, NCH_3), 1.82–1.04 ppm (m, 8H, CH_{2Ach}); ^{13}C NMR ($CDCl_3$, 75.40 MHz): δ=175.1 (CO), 171.3 (CO), 136.5 (C), 129.6 (CH), 128.2 (CH), 126.8 (CH), 51.4 (CH), 49.9 (CH), 43.3 (CH), 40.4 (CH_2), 30.8 (CH_2), 30.1 (CH_2), 29.5 (NCH_3), 28.5 (CH_2), 24.7 ppm (CH_2); FT-IR (293 K, $CHCl_3$): $\tilde{\nu}$=3312 (amide A), 2935, 2864, 1660, 1623 (amide I), 1525 cm^{-1} (amide II$_{II}$); MS (FAB$^+$): *m/z* (%): 1145 ([*M*H]$^+$, 100); HRMS (FAB$^+$): calcd for $C_{68}H_{89}N_8O_8$ ([*M*H]$^+$): 1145.68034; found: 1145.68176.

Synthesis of *cyclo*{[D-Ser(Bn)-L-^{Me}N-γ-Ach]$_4$-} (10b): Prepared from Boc-{[D-Ser(Bn)-L-^{Me}N-γ-Ach]$_4$-}OFm (99 mg, 78 μmol) in the same way as **9** to yield, after HPLC purification, CP **10b** (50 mg, 50%); white solid. ^{1}H NMR ($CDCl_3$, 250.13 MHz): δ=8.41 (d, J=8.4 Hz, 1H, NH_{Ser}), 7.32–7.10 (m, 5H, Ar-H_{Bn}), 5.39 (dd, J=21.8 Hz, 1H, Hα_{Ser}), 4.54 (m, 1H, Hγ_{Ach}), 4.37 (overlapping doublets, J=8.0 Hz, 2H, CH_2Bn), 3.61–3.42 (m, 2H, $CH_2\beta_{Ser}$), 3.04 (s, 3H, NCH_3), 2.84 (m, 1H, Hα_{Ach}) 1.92–1.21 ppm (m, 8H, CH_{2Ach}); ^{13}C NMR ($CDCl_3$, 62.90 MHz): δ=175.4 (CO), 170.6 (CO), 137.9 (C), 128.2 (CH), 127.5 (CH), 127.1 (CH), 73.1 (CH_2), 71.4 (CH_2), 51.7 (CH), 47.9 (CH), 43.2 (CH), 31.1 (CH_2), 29.9 (NCH_3), 29.8 (CH_2), 28.7 (CH_2), 24.6 ppm (CH_2); FT-IR (293 K, $CHCl_3$): $\tilde{\nu}$=3309 (amide A), 2936, 2863, 1660, 1628 (amide I), 1524 cm^{-1} (amide II$_{II}$); MS (FAB$^+$): *m/z* (%): 1265 ([*M*H]$^+$, 100); HRMS (FAB$^+$): calcd for $C_{72}H_{96}N_8O_{12}$ ([*M*H]$^+$): 1265.72260; found: 1265.72583.

Synthesis of *cyclo*[(D-Ser-L-^{Me}N-γ-Ach)$_4$-] (10c): A solution of *cyclo*{[D-Ser(Bn)-L-^{Me}N-γ-Ach]$_4$-} (**10b**; 50 mg, 40 μmol) in EtOH (1.5 mL) was treated with 10% Pd/C (12 mg, 11 μmol) and stirred at RT under hydrogen overnight. The resulting mixture was filtered through a Celite pad, the residue was washed with ethanol, and the combined filtrates and washings were concentrated under reduced pressure to afford **10c** as a white solid (36 mg, 99%). ^{1}H NMR ([D$_6$]DMSO, 250.13 MHz): δ=8.14–7.87 (m, 1H, NH_{Ser}), 4.71 (m, 1H, Hα_{Ser}), 4.27 (m, 1H, Hγ_{Ach}), 3.40 (m, 2H, $CH_2\beta_{Ser}$), 2.88 (m, 1H, Hα_{Ach}), 2.86 (s, 3H, NCH_3), 1.72–1.22 ppm (m, 8H, CH_{2Ach}); ^{13}C NMR ($CDCl_3$, 62.90 MHz): δ=174.0 (CO), 169.8 (CO), 61.8 (CH_2), 51.2 (CH), 42.7 (CH), 39.7 (CH), 31.3 (CH_2), 29.1 (NCH_3), 29.0 (CH_2), 28.5 (CH_2), 24.3 ppm (CH_2); FT-IR (293 K, CaF_2): $\tilde{\nu}$=3310 (amide A), 2933, 2864, 1661, 1621 (amide I), 1541 cm^{-1} (amide II$_{II}$); MS (FAB$^+$): *m/z* (%): 905 ([*M*H]$^+$, 100); HRMS (FAB$^+$): calcd for $C_{44}H_{73}N_8O_{12}$ ([*M*H]$^+$): 905.53480; found: 905.53476.

Synthesis of *cyclo*{[D-Phe-L-^{Me}N-γ-Ach-D-Ser(Bn)-L-^{Me}N-γ-Ach]$_2$-} (11a)[7c]: Previously obtained from Boc-{[D-Phe-L-^{Me}N-γ-Ach-D-Ser(Bn)-L-^{Me}N-γ-Ach]$_2$-}-OFm (100.0 mg, 66.7 μmol) in the same way as **9** to yield, after HPLC purification, CP **11a** (73.4 mg, 92%); white solid. ^{1}H NMR ($CDCl_3$, 750.00 MHz): δ=8.59 (d, J=8.2 Hz, 2H, NH_{Ser} **D_{11a}[A]**), 8.52 (overlapping doublets, J=9.4 Hz, 2.14H, NH_{Phe} **D_{11a}[E]**+NH_{Phe} **D_{11a}[A]**), 8.29 (d, J=8.4 Hz, 0.14H, NH_{Ser} **D_{11a}[E]**), 7.23–7.06 (m, 21.4H, Ar_{Phe}+Ar_{Bn}), 5.35–5.29 (m, 2.14H, Hα_{Ser}), 5.22–5.14 (m, 2.14H, Hα_{Phe}), 4.52–4.37 (m, 4.28H, Hγ_{Ach}), 4.32 (d, J=3.3 Hz, 4.28H, CH_{2Bn}), 3.61–3.54 (m, 2.14H, $CH_2\beta_{Ser}$), 3.50–3.45 (m, 2.14H, $CH_2\beta_{Ser}$), 3.19–2.93 (m, 6.42H, Hα_{Ach}+$CH_2\beta_{Phe}$), 2.91 (s, 6.42H, NCH_3), 2.85–2.77 (m, 2.14H, $CH_2\beta_{Phe}$), 2.74 (s, 6.42H, NCH_3), 2.45–2.35 (m, 4.28H, CH_{2Ach}), 1.92–0.91 ppm (29.96H, CH_{2Ach}); ^{13}C NMR ($CDCl_3$, 75.40 MHz):

δ = 175.9 (CO), 174.5 (CO), 171.5 (CO), 169.9 (CO), 137.6 (C), 137.2 (C), 127.8 (CH), 127.2 (CH), 126.5 (CH), 125.4 (CH), 73.2 (CH_2), 71.6 (CH_2), 51.9 (CH), 51.0 (CH), 49.8 (CH), 48.5 (CH), 44.2 (CH), 42.4 (CH), 38.9 (CH_2), 31.8 (CH_2), 31.0 (CH_2), 30.3 (CH_3), 29.9 (CH_3), 29.6 (CH_3), 28.7 (CH_2), 28.4 (CH_2), 24.6 ppm (CH_2); FT-IR (293 K, $CHCl_3$): $\tilde{\nu}$ = 3311 (amide A), 2934, 2861, 1660, 1625 (amide I), 1523 cm^{-1} (amide II_{II}); MS (ESI): *m*/*z* (%): 1227 ([*M*+Na]$^+$, 46) 1205 ([*M*H]$^+$, 100); HRMS (ESI): calcd for $C_{70}H_{93}N_8O_{10}$ ([*M*H]$^+$): 1205.7015; found: 1205.7009.

Synthesis of *cyclo*[(D-Phe-L-^{Me}N-γ-Ach-D-Ser-L-^{Me}N-γ-Ach)$_2$-] (11b)[7c]: A solution of *cyclo*{[D-Phe-L-^{Me}N-γ-Ach-D-Ser(Bn)-L-^{Me}N-γ-Ach]$_2$-} (**11a**, 20.0 mg, 16.6 μmol) in EtOH (250 μL) was treated with 10% Pd/C (3.5 mg, 3.3 μmol) and stirred overnight at RT under a hydrogen atmosphere. The resulting mixture was filtered through a Celite pad, the residue was washed with ethanol, and the combined filtrates and washings were concentrated under reduced pressure to afford **11b** as a white solid (16.2 mg, 95%). ^{1}H NMR ($CDCl_3$, 750.00 MHz): δ = 8.96 (s, 2H, NH_{Ser} **D_{11b}[A]**), 8.65 (brs, 0.32H, NH_{Phe} **D_{11b}[E]**), 8.49 (d, *J* = 9.8 Hz, 2H, NH_{Phe} **D_{11b}[A]**), 8.14 (brs, 0.32H, NH_{Ser} **D_{11b}[E]**), 7.24–7.08 (m, 11.6H, Ar-H_{Phe}), 5.31–5.24 (m, 2.32H, Hα_{Ser}), 5.22–5.16 (m, 2.32H, Hα_{Phe}), 4.52–4.45 (m, 4.64H, Hγ_{Ach}), 3.89–3.81 (m, 2.32H, $CH_2\beta_{Ser}$), 3.76–3.69 (m, 2.32H, $CH_2\beta_{Ser}$), 3.32–3.25 (m, 4.64H, Hα_{Ach}), 3.09–3.01 (m, 9.28H, NCH_3+$CH_2\beta_{Phe}$), 2.97–2.90 (m, 2.32H, $CH_2\beta_{Phe}$), 2.80 (s, 6.96H, NCH_3), 2.45–2.39 (m, 4.64H, CH_{2Ach}), 1.92–1.03 (m, 34.8H, CH_{2Ach}+OH_{Ser}); ^{13}C NMR ($CDCl_3$, 75.40 MHz): δ = 177.9 (CO), 174.2 (CO), 171.8 and 171.6 (CO), 168.6 and 168.6 (CO), 136.8 and 136.8 (C), 129.8 (CH), 128.2 (CH), 126.7 (CH), 67.0 (CH_2), 53.3 (CH), 52.2 (CH), 51.2 (CH), 50.0 (CH), 44.4 (CH), 42.5 (CH), 39.3 (CH_2), 32.2 and 32.1 (CH_2), 30.8 (CH_2), 29.9 and 29.8 (CH_3), 29.1, 28.7 and 28.6 (CH_2), 24.7 ppm (CH_2); FTIR (293 K, $CHCl_3$): $\tilde{\nu}$ = 3317 (amide A), 2935, 2863, 1660, 1620 (amide I), 1524 cm^{-1} (amide II_{II}); MS (FAB$^+$): *m*/*z* (%): 1025 ([*M*H]$^+$, 100); HRMS (FAB$^+$): calcd for $C_{56}H_{81}N_8O_{10}$ ([*M*H]$^+$): 1025.60757; found: 1025.60908.

Synthesis of *cyclo*{[D-Phe-L-^{Me}N-γ-Ach-D-Ser(Pyr)-L-^{Me}N-γ-Ach]$_2$-} (11c): A solution of 1-pyreneacetic acid (3.3 mg, 12.7 μmol) in $CDCl_3$ (500 μL) was stirred and sonicated at RT for 10 min, after which DIC (3.0 μL, 19.1 μmol), *cyclo*[(D-Phe-L-^{Me}N-γ-Ach-D-Ser-L-^{Me}N-γ-Ach)$_2$-] (**11b**, 6.5 mg, 6.4 μmol), and DMAP (2.3 mg, 19.1 μmol) were successively added. The mixture was stirred for 1 h and the solution was washed with HCl (5%) and $NaHCO_3$ (sat.), dried over Na_2SO_4, and concentrated under reduced pressure. The residue was purified by flash chromatography (0–7% MeOH in CH_2Cl_2) to give **11c** as a yellow solid [9.1 mg, 95%, R_f = 0.37 (3% MeOH in CH_2Cl_2)]. ^{1}H NMR ($CDCl_3$, 500.13 MHz): δ = 8.55 (d, *J* = 7.8 Hz, 2H, NH_{Ser} **D_{11c}[A]**), 8.36 (d, *J* = 8.0 Hz, 0.20H, NH_{Phe} **D_{11c}[E]**), 8.29 (d, *J* = 9.5 Hz, 2H, NH_{Phe} **D_{11c}[A]**), 8.19–7.88 (m, 17.8H, NH_{Ser} **D_{11c}[E]**+Ar-H_{Pyr}), 7.80 (overlapping doublets, *J* = 7.8 Hz, 2.2H, Ar-H_{Pyr}), 7.16–7.01 (m, 11H, Ar_{Phe}), 5.44–5.33 (m, 2H, Hα_{Ser} **D_{11c}[A]**), 5.25–5.13 (m, 2.4H, Hα_{Phe} **D_{11c}[E]**+Hα_{Phe} **D_{11c}[A]**+Hα_{Ser} **D_{11c}[E]**), 4.42–4.31 (m, 2.2H, Hγ_{Ach}), 4.29–4.12 (m, 8.8H, $CH_2\beta_{Ser}$+CH_{2Pyr}+Hγ_{Ach}), 3.98–3.89 (m, 2.2H, $CH_2\beta_{Ser}$), 3.10–2.95 (m, 4.4H, Hα_{Ach}+$CH_2\beta_{Phe}$), 2.91–2.83 (m, 2.2H, $CH_2\beta_{Phe}$), 2.75 (overlapping singlets, 6.6H, NCH_3), 2.68 (overlapping singlets, 6.6H, NCH_3), 2.58–2.48 (m, 2.2H, Hα_{Ach}), 2.25–2.12 (m, 2.2H, CH_{2Ach}), 1.79–1.68 (m, 2.2H, CH_{2Ach}), 1.66–0.68 ppm (30.8H, CH_{2Ach}); MS (MALDI-TOF): *m*/*z* (%): 1548 ([*M*+K]$^+$, 12), 1532 ([*M*+Na]$^+$, 100), 1509 ([*M*H]$^+$, 17); HRMS (MALDI-TOF): calcd for $C_{92}H_{101}N_8O_{12}$ ([*M*H]$^+$): 1509.75; found: 1509.74.

Synthesis of *cyclo*{[D-Phe-L-^{Me}N-γ-Acp-D-Ser(Bn)-L-^{Me}N-γ-Acp]$_2$-} (12a): A solution of Boc-[D-Phe-L-^{Me}N-γ-Acp-D-Ser(Bn)-L-^{Me}N-γ-Acp]-OFm (200.0 mg, 0.23 mmol) in 20% piperidine in DCM (2.3 mL) was stirred at RT for 20 min. The solvent was removed and the residue was dissolved in DCM (10 mL). The solution was washed with HCl (5%), dried over Na_2SO_4, filtered, and concentrated. The resulting residue was dissolved in TFA/DCM (2.3 mL, 1:1) and the solution was stirred at RT for 15 min. The solvent was removed and the residue was dried under high vacuum for 3 h and used without further purification. The linear peptide was dissolved in DCM (46 mL) and treated with HATU (104.9 mg, 0.28 mmol), followed (dropwise) by DIEA (160.6 μL, 0.92 mmol) [an additional 1 equiv of HATU (87.4 mg, 0.23 mmol) and 4 equiv of DIEA (160.6 μL, 0.92 mmol) were added when the starting material was observed by HPLC]. The resulting mixture was stirred for 3 h at RT to complete the reaction. After 12 h, the solvent was removed under reduced pressure and the crude product was purified by HPLC to afford **11a** as a white foam [40.7 mg, 31%, R_t = 18 min (Phenomenex Maxsil-10 semipreparative column, 3–12% MeOH in CH_2Cl_2, 25 min)]. ^{1}H NMR ($CDCl_3$, 500.13 MHz): δ = 8.66 (d, *J* = 9.0 Hz, 2H, NH_{Phe} **D_{12a}[E]**), 8.52 (d, *J* = 8.6 Hz, 2H, NH_{Ser} **D_{12a}[A]**), 8.48 (d, *J* = 9.2 Hz, 2H, NH_{Phe} **D_{12a}[A]**), 8.27 (d, *J* = 9.1 Hz, 2H, NH_{Ser} **D_{12a}[E]**), 7.25–7.02 (m, 40H, Ar-H_{Phe}+Ar-H_{Bn}), 5.41–5.09 (m, 8H, Hα_{Ser}+Hα_{Phe}), 4.94–4.65 (m, 8H, Hγ_{Acp}), 4.44 (d, *J* = 12.5 Hz, 2H, CH_{2Bn}), 4.41–4.35 (overlapping doublets, *J* = 12.4 Hz, 4H, CH_{2Bn}), 4.21 (d, *J* = 12.5 Hz, 2H, CH_{2Bn}), 3.59 (m, 4H, $CH_2\beta_{Ser}$ **D_{12a}[A]**), 3.27 (m, 4H, $CH_2\beta_{Ser}$ **D_{12a}[E]**), 3.17–2.84 (m, 24H, Hα_{Acp}+$CH_2\beta_{Phe}$ **D_{12a}[E]**+NCH_3), 2.77 (m, 4H, $CH_2\beta_{Phe}$ **D_{12a}[A]**), 2.47 (m, 12H, NCH_3), 2.02–0.76 ppm (m, 48H, CH_{2Acp}); ^{13}C NMR ($CDCl_3$, 125.77 MHz): δ = 174.8 (CO), 174.4 (CO), 172.3 (CO), 171.5 (CO), 137.9 (C), 136.6 (C), 129.3 (CH), 128.3 (CH), 128.2 (CH), 127.5 (CH), 127.1 (CH), 126.9 (CH), 72.8 (CH_2), 71.0 (CH_2), 54.6 (CH), 54.2 (CH), 50.0 (CH), 48.1 (CH), 42.6 (CH), 42.3 (CH), 40.6 (CH_2), 33.3 (CH_2), 29.7 (CH_3), 29.1 (CH_3), 27.6 (CH_2), 27.3 (CH_2), 26.8 (CH_2), 26.6 (CH_2), 26.4 (CH_2), 26.0 ppm (CH_2); MS (ESI): *m*/*z* (%): 1172 ([*M*+Na]$^+$, 2), 1149 ([*M*H]$^+$, 6), 594 ([*M*+K]$^{2+}$, 100); HRMS (ESI): calcd for $C_{66}H_{85}N_8O_{10}$ ([*M*H]$^+$): 1149.6383; found: 1149.6398.

Synthesis of *cyclo*[(D-Phe-L-^{Me}N-γ-Acp-D-Ser-L-^{Me}N-γ-Acp)$_2$-] (12b): Anisole (12.4 μL, 0.13 μmol), pentamethylbenzene (12.2 mg, 82.5 μmol), TFA (1.85 mL), and HBr solution (33% in AcOH, 400 μL) were successively added to *cyclo*{[D-Phe-L-^{Me}N-γ-Acp-D-Ser(Bn)-L-^{Me}N-γ-Acp]$_2$-} (**12a**, 12.0 mg, 10.4 μmol). The resulting mixture was vigorously stirred for 2 h at RT and then evaporated to dryness in vacuo to give **12b** as an orange oil, which was used without further purification [10.1 mg, 100%]. MS (ESI): *m*/*z* (%): 992 ([*M*+Na]$^+$, 16), 969 ([*M*H]$^+$, 100); HRMS (ESI): calcd for $C_{52}H_{72}N_8O_{10}$ ([*M*H]$^+$): 969.5444; found: 969.5459.

Synthesis of *cyclo*{[D-Phe-L-^{Me}N-γ-Acp-D-Ser(Pyr)-L-^{Me}N-γ-Acp]$_2$-} (12c): A solution of 1-pyreneacetic acid (5.4 mg, 20.9 μmol) in DMF/$CDCl_3$ (1:4) (500 μL) was stirred and sonicated at RT for 10 min, and then DIC (2.5 μL, 15.7 μmol), *cyclo*[(D-Phe-L-^{Me}N-γ-Acp-D-Ser-L-^{Me}N-γ-Acp)$_2$-] (**12b**, 10.1 mg, 10.4 μmol), and DMAP (1.9 mg, 15.7 μmol) were successively added. The mixture was stirred for 1 h at RT, the solution was then washed with HCl (5%) and $NaHCO_3$ (sat.), dried over Na_2SO_4, and concentrated under reduced pressure. The residue was purified by HPLC to give **12c** as a yellow solid [3.5 mg, 23%, R_t = 23 min (Phenomenex Maxsil-10 semipreparative column, 0–15% MeOH in CH_2Cl_2, 30 min)]. ^{1}H NMR ($CDCl_3$, 500.13 MHz): δ = 8.55 (d, *J* = 9.4 Hz, 2H, NH_{Phe} **D_{12c}[E]**), 8.47 (d, *J* = 9.0 Hz, 2H, NH_{Ser} **D_{12c}[A]**), 8.16 (d, *J* = 9.4 Hz, 2H, NH_{Phe} **D_{12c}[A]**), 8.14–7.86 (m, 30H, NH_{Ser} **D_{12c}[E]**+Ar-H_{Pyr}), 7.81 (d, *J* = 8.0 Hz, 2H, Ar-H_{Pyr}), 7.74 (d, *J* = 7.9 Hz, 2H, Ar-H_{Pyr}), 7.64 (m, 2H, Ar-H_{Pyr}), 7.46 (m, 2H, Ar-H_{Pyr}), 7.17–7.00 (m, 20H, Ar_{Phe}), 5.39–4.97 (m, 16H, Hα_{Ser}+Hα_{Phe}+CH_{2Pyr}), 4.74–4.41 (m, 8H, Hγ_{Acp}), 4.38–3.76 (m, 8H, $CH_2\beta_{Ser}$), 3.08–2.63 (m, 8H, $CH_2\beta_{Phe}$), 2.61–0.56 ppm (m, 80H, Hγ_{Acp}+NCH_3+CH_{2Acp}); MS (ESI): *m*/*z* (%): 746 ([*M*+K]$^{2+}$, 100), 738 ([*M*+Na]$^{2+}$, 26); HRMS (ESI): calcd for $C_{88}H_{92}N_8O_{12}Na$ ([*M*+Na]$^{2+}$): 738.3400; found: 738.3395.

Synthesis of *cyclo*{[D-Phe-L-^{Me}N-γ-Acp-D-Glu(Bn)-L-^{Me}N-γ-Acp]$_2$-} (12d): Prepared from Boc-[D-Phe-L-^{Me}N-γ-Acp-D-Glu(Bn)-L-^{Me}N-γ-Acp-]OFm (1000.0 mg, 1.09 mmol) in the same way as **11a** to yield, after HPLC purification, the desired CP (254.1 mg, 38%); white foam. ^{1}H NMR ($CDCl_3$, 500.13 MHz): δ = 8.65 (d, *J* = 8.9 Hz, 1.7H, NH_{Phe} **D_{12d}[E]**), 8.54 (d, *J* = 9.0 Hz, 2H, NH_{Glu} **D_{12d}[A]**), 8.30 (d, *J* = 9.0 Hz, 2H, NH_{Phe} **D_{12d}[A]**), 8.16 (d, *J* = 9.0 Hz, 1.7H, NH_{Glu} **D_{12d}[E]**), 7.29–7.05 (m, 37H, Ar-H_{Phe}+Ar-H_{Bn}), 5.28–5.15 (m, 3.7H, Hα_{Phe} **D_{12d}[E]**+Hα_{Phe} **D_{12d}[A]**), 5.13–5.06 (m, 2H, Hα_{Glu} **D_{12d}[A]**), 5.05–5.00 (m, 5.7H, Hα_{Glu} **D_{12d}[E]**+CH_{2Bn} **D_{12d}[A]**), 4.98–4.96 (overlapping singlets, 3.4H, CH_{2Bn} **D_{12d}[E]**), 4.83–4.62 (m, 7.4H, Hγ_{Acp}), 3.08–2.76 (m, 25.9H, Hα_{Acp}+$CH_2\beta_{Phe}$+NCH_3), 2.53–2.19 (m, 18.5, NCH_3+$CH_2\gamma_{Glu}$), 2.08–1.09 ppm (m, 51.8H, $CH_2\beta_{Glu}$+CH_{2Acp}); ^{13}C NMR ($CDCl_3$, 125.77 MHz): δ = 175.0 (CO), 174.5 (CO), 172.5 (CO), 172.3 (CO), 172.1 (CO), 136.5 (C), 135.8 (C), 129.3 (CH), 128.5 (CH), 128.4 (CH), 128.3 (CH), 128.2 (CH), 126.9 (CH), 66.4 (CH_2), 54.7 (CH), 54.4 (CH), 50.2 (CH), 47.7

(CH), 42.4 (CH), 42.2 (CH), 40.8 (CH_2), 34.0 (CH_2), 33.2 (CH_2), 33.0 (CH_2), 30.0 (CH_2), 29.8 (CH_3), 29.5 (CH_2), 29.3 (CH_2), 29.2 (CH_2), 29.0 (CH_3), 28.8 (CH_2), 28.6 (CH_2), 28.0 (CH_2), 27.7 (CH_2), 27.5 (CH_2), 27.2 (CH_2), 26.9 (CH_2), 26.4 (CH_2), 26.0 ppm (CH_2); MS (MALDI-TOF): *m/z* (%): 1272 ([*M*+K]$^+$, 2), 1256 ([*M*+Na]$^+$, 57), 1234 ([*M*H]$^+$, 100); HRMS (MALDI-TOF): calcd for $C_{70}H_{89}N_8O_{12}$ ([*M*H]$^+$): 1233.6600; found: 1233.6639.

Synthesis of *cyclo*[(D-Phe-L-^{Me}N-γ-Acp-D-Glu-L-^{Me}N-γ-Acp)$_2$-] (12e): A solution of *cyclo*{[D-Phe-L-^{Me}N-γ-Acp-D-Glu(Bn)-L-^{Me}N-γ-Acp]$_2$-} (**12d**, 50.0 mg, 40.6 μmol) in 5% AcOH in CH_2Cl_2 (1 mL) was treated with 10% Pd/C (8.6 mg, 8.1 μmol) and stirred at RT under hydrogen overnight. The resulting mixture was filtered through a Celite pad, the residue was washed with MeOH/CH_2Cl_2 (1:1) and the combined filtrates and washings were concentrated under reduced pressure to afford **12e** as a white solid (40.2 mg, 94%); MS (ESI-TOF): *m/z* (%): 1075 ([*M*+Na]$^+$, 24), 1053 ([*M*H]$^+$, 100), 527 ([*M*H]$^{2+}$, 68); HRMS (ESI-TOF): calcd for $C_{56}H_{77}N_8O_{12}$ ([*M*H]$^+$): 1053.566091; found: 1053.563722.

Synthesis of *cyclo*{[D-Phe-L-^{Me}N-γ-Acp-D-Glu(Per)-L-^{Me}N-γ-Acp]$_2$-} (12f): A solution of *cyclo*[(D-Phe-L-^{Me}N-γ-Ach-D-Glu-L-^{Me}N-γ-Acp)$_2$-] (**12e**, 30.0 mg, 28.5 μmol) in DMF/$CDCl_3$ (1:11, 3.0 mL) was stirred and sonicated at RT for 10 min and then DIC (3.0 μL, 19.1 μmol), perylen-3-ylmethanol (**14**, 24.1 mg, 85.6 μmol), and DMAP (15.7 mg, 128.3 μmol) were successively added. The mixture was stirred for 1 h at RT and the solution was washed with HCl (5%) and $NaHCO_3$ (sat.), dried over Na_2SO_4, and concentrated under reduced pressure. The residue was purified by HPLC to give **12f** as a yellow solid [26.3 mg, 58%, R_t = 17 min (Phenomenex Maxsil-10 semipreparative column, 0–10% MeOH in CH_2Cl_2, 30 min)]. ^{1}H NMR ($CDCl_3$, 500.13 MHz): δ = 8.62 (d, *J* = 8.9 Hz, 2H, NH_{Phe} **D$_{12f}$[E]**), 8.53 (d, *J* = 8.7 Hz, 1.3H, NH_{Glu} **D$_{12f}$[A]**), 8.28 (d, *J* = 8.8 Hz, 1.3H, NH_{Phe} **D$_{12f}$[A]**), 8.17 (d, *J* = 8.8 Hz, 2H, NH_{Glu} **D$_{12f}$[E]**), 8.14–7.25 (overlapping doublets+doublets, 36.3H, Ar-H_{Per}), 7.18–6.99 (m, 16.5H, Ar-H_{Phe}), 5.38 (d, *J* = 1.6 Hz, 2.6H, CH_{2Per} **D$_{12f}$[A]**), 5.29 (d, *J* = 6.5 Hz, 4H, CH_{2Per} **D$_{12f}$[E]**), 5.20 (m, 2H, Hα_{Phe} **D$_{12f}$[E]**), 5.18–5.08 (m, 2.6H, Hα_{Glu} **D$_{12f}$[S]**+Hα_{Phe} **D$_{12f}$[A]**), 5.04 (m, 2H, Hα_{Glu} **D$_{12f}$[E]**), 4.83–4.55 (m, 6.6H, Hγ_{Acp}), 3.07–2.83 (m, 23.1H, Hα_{Acp}+$CH_2\beta_{Phe}$+NCH_3), 2.51–2.17 (m, 16.5, NCH_3+$CH_2\gamma_{Glu}$), 2.04–1.03 ppm (m, 46.2H, $CH_2\beta_{Glu}$+CH_{2Acp}); MS (MALDI-TOF): *m/z* (%): 1619 ([*M*+K]$^+$, 52), 1603 ([*M*+Na]$^+$, 50), 1581 ([*M*H]$^+$, 2); HRMS (MALDI-TOF): calcd for $C_{98}H_{100}N_8O_{12}K$ ([*M*+K]$^+$): 1619.7098; found: 1619.7094.

Time-Resolved Fluorescence

Fluorescence lifetimes were determined by time-correlated single-photon counting by using an Edinburgh Instruments CD-900 spectrometer equipped with a hydrogen-filled nanosecond flash lamp. The instrumental response width of the system was 1.0 ns. Measurements were usually carried out until 10000 counts were reached in (2×10^3 channels). The emission band-pass for the lifetime measurements was usually 20 nm. The experiments were performed at room temperature and samples were purged with argon prior to measurement.

Acknowledgements

This work was supported in part by the Spanish Ministry of Science and Innovation (Micinn), ERDF [under projects SAF2007-61015 and Consolider Ingenio 2010 (CSD2007-00006)], the European project Magnifyco (NMP4-SL-2009-228622) and the Xunta de Galicia (PGIDIT08C-SA047209PR and R2006/124). R.J.B. and M.J.P.-A. thank the Spanish M.E.C. for their FPU and FPI fellowships, respectively. M.P. thanks Spanish M.A.E.C. for her MAEC-AECI fellowship.

[1] a) T. Brixner, J. Stenger, H. M. Vaswani, M. Cho, R. E. Blankenship, G. R. Fleming, *Nature* **2005**, *434*, 625–628; b) L. M. Yoder, A. G. Cole, R. J. Sension, *Photosynth. Res.* **2002**, *72*, 147–158; c) T. Pullerits, V. Sundström, *Acc. Chem. Res.* **1996**, *29*, 381–389; d) M. R. Wasielewski, *Chem. Rev.* **1992**, *92*, 435–461; e) R. Huber, *Angew. Chem.* **1989**, *101*, 849–871; *Angew. Chem. Int. Ed. Engl.* **1989**, *28*, 848–869.

[2] For light harvesting energy-transfer system based on synthetic protein assemblies, see; a) R. A. Miller, A. D. Presley, M. B. Francis, *J. Am. Chem. Soc.* **2007**, *129*, 3104–3109; b) M. Endo, M. Fujitsuka, T. Majima, *Chem. Eur. J.* **2007**, *13*, 8660–8666; c) Y. Z. Hu, S. Tsukiji, S. Shinkai, S. Oishi, I. Hamachi, *J. Am. Chem. Soc.* **2000**, *122*, 241–253.

[3] a) E. R. Young, J. Rosenthal, J. M. Hodgkiss, D. G. Nocera, *J. Am. Chem. Soc.* **2009**, *131*, 7678–7684; b) G. Fernández, E. M. Pérez, L. Sánchez, N. Martín, *Angew. Chem.* **2008**, *120*, 1110–1113; *Angew. Chem. Int. Ed.* **2008**, *47*, 1094–1097; c) P. G. A. Janssen, J. Vandenbergh, J. L. J. Van Dongen, E. W. Meijer, A. P. H. J. Schenning, *J. Am. Chem. Soc.* **2007**, *129*, 6078–6079; d) A. Del Guerzo, A. G. L. Olive, J. Reichwagen, H. Hopf, J. P. Desvergne, *J. Am. Chem. Soc.* **2005**, *127*, 17984–17985.

[4] a) R. J. Brea, C. Reiriz, J. R. Granja, *Chem. Soc. Rev.* **2010**, *39*, 1448–1456; b) R. J. Brea, J. R. Granja in *Dekker Encyclopedia of Nanoscience and Nanotechnology* (Eds: J. A. Schwarz, C. I. Contescu, K. Putyera), Marcel Dekker Inc, New York, **2004**, pp. 3439–3457; c) G. R. Patzke, F. Krumeich, R. Nesper, *Angew. Chem.* **2002**, *114*, 2554–2571; *Angew. Chem. Int. Ed.* **2002**, *41*, 2446–2461; d) D. T. Bong, T. D. Clark, J. R. Granja, M. R. Ghadiri, *Angew. Chem.* **2001**, *113*, 1016–1041; *Angew. Chem. Int. Ed.* **2001**, *40*, 988–1011.

[5] a) V. Gauba, J. D. Hartgerink, *J. Am. Chem. Soc.* **2007**, *129*, 2683–2690; b) E. S. Barrett, T. J. Dale, J. Rebek, Jr., *J. Am. Chem. Soc.* **2007**, *129*, 8818–8824; c) W. Zheng, H. O. Jacobs, *Adv. Funct. Mater.* **2005**, *15*, 732–738; d) M. V. Ovchinnikov, A. M. Brown, X. Liu, C. A. Mirkin, L. N. Zakharov, A. L. Rheingold, *Inorg. Chem.* **2004**, *43*, 8233–8235.

[6] a) P. M. Bowers, S. J. Cokus, D. Eisenberg, T. O. Yeates, *Science* **2004**, *306*, 2246–2249; b) A. Tsuchisaka, A. Theologis, *Proc. Natl. Acad. Sci. USA* **2004**, *101*, 2275–2280; c) S. K. Nair, S. K. Burley, *Cell* **2003**, *112*, 193–205; d) D. W. Felsher, *Nat. Rev. Cancer* **2003**, *3*, 375–380; e) M. R. Young, H.-S. Yang, N. H. Colburn, *Trends Mol. Med.* **2003**, *9*, 36–41; f) R. Eferl, R. Ricci, L. Kenner, R. Zenz, J.-P. David, M. Rath, E. F. Wagner, *Cell* **2003**, *112*, 181–192.

[7] a) C. Reiriz, M. Amorín, R. García-Fandiño, L. Castedo, J. R. Granja, *Org. Biomol. Chem.* **2009**, *7*, 4358–4361; b) R. J. Brea, L. Castedo, J. R. Granja, *Chem. Commun.* **2007**, 3267–3269; c) M. Amorín, L. Castedo, J. R. Granja, *Chem. Eur. J.* **2005**, *11*, 6543–6551; d) M. Amorín, R. J. Brea, L. Castedo, J. R. Granja, *Org. Lett.* **2005**, *7*, 4681–4684; e) M. Amorín, L. Castedo, J. R. Granja, *J. Am. Chem. Soc.* **2003**, *125*, 2844–2845.

[8] M. Amorín, L. Castedo, J. R. Granja, *Chem. Eur. J.* **2008**, *14*, 2100–2111.

[9] For α,γ-peptide nanotube formation, see: a) R. García-Fandiño, J. R. Granja, D. A. Marco, M. Orozco, *J. Am. Chem. Soc.* **2009**, *131*, 15678–15686; b) C. Reiriz, R. J. Brea, R. Arranz, J. L. Carrascosa, A. Garibotti, B. Manning, J. M. Valpuesta, R. Eritja, L. Castedo, J. R. Granja, *J. Am. Chem. Soc.* **2009**, *131*, 11335–11337.

[10] R. J. Brea, M. Amorín, L. Castedo, J. R. Granja, *Angew. Chem.* **2005**, *117*, 5856–5859; *Angew. Chem. Int. Ed.* **2005**, *44*, 5710–5713.

[11] For theoretical studies carried out with homo-and heterodimers, see: R. García-Fandiño, L. Castedo, J. R. Granja, S. Vázquez, *J. Phys. Chem. B* **2010**, *114*, 4973–4983.

[12] For heteromeric peptide nanotube formation driven mainly by side-chain/side-chain interactions, see: a) K. Rosenthal-Aizman, G. Svensson, A. Undén, *J. Am. Chem. Soc.* **2004**, *126*, 3372–3373; b) J. Sánchez-Quesada, M. P. Isler, M. R. Ghadiri, *J. Am. Chem. Soc.* **2002**, *124*, 10004–10005.

[13] For donor-acceptor systems based on α,γ-CP heterodimer formation, see: a) R. J. Brea, M. A. Herranz, L. Sánchez, L. Castedo, W. Seitz, D. M. Guldi, N. Martín, J. R. Granja, *Proc. Natl. Acad. Sci. USA* **2007**, *104*, 5291–5294; b) R. J. Brea, M. E. Vázquez, M. Mosquera, L. Castedo, J. R. Granja, *J. Am. Chem. Soc.* **2007**, *129*, 1653–1657.

[14] a) J. J. Havranek, P. B. Harbury, *Nat. Struct. Biol.* **2003**, *10*, 45–52; b) A. Apelblat, *Can. J. Chem.* **1991**, *69*, 638–647.

[15] S. Krimm, J. Bandekar in *Advances in Protein Chemistry* (Eds: C. B. Anfinsen, J. T. Edsall, F. M. Richards), Academic Press, Orlando, **1986**, pp. 181–364.
[16] M. Amorin, V. Villaverde, L. Castedo, J. R. Granja, *J. Drug Delivery Sci. Technol.* **2005**, *15*, 87–92.
[17] For a recent studies of molecular tweezers based on α,γ-CP dimer/porphyrin hybrids, see: L. P. Hernández-Eguía, R. J. Brea, L. Castedo, P. Ballester, J. R. Granja *Chem. Eur. J.* **2010**, DOI:10.1002/chem.201002271.
[18] a) V. A. Azov, A. Schlegel, F. Diederich, *Angew. Chem.* **2005**, *117*, 4711–4715; *Angew. Chem. Int. Ed.* **2005**, *44*, 4635–4638; b) Y. Kanekiyo, R. Naganawa, H. Tao, *Chem. Commun.* **2004**, 1006–1007; c) R. B. Martin, K. Fu, H. Li, D. Cole, Y.-P. Sun, *Chem. Commun.* **2003**, 2368–2369.
[19] a) N. Ashkenasy, W. S. Horne, M. R. Ghadiri, *Small* **2006**, *2*, 99–102; b) W. S. Horne, N. Ashkenasy, M. R. Ghadiri, *Chem. Eur. J.* **2005**, *11*, 1137–1144.
[20] For pyrene/perylene FRET pair, see: a) D. Lindegaard, A. S. Madsen, I. V. Astakhova, A. D. Malakhov, B. R. Babu, V. A. Korshunb, J. Wengel, *Bioorg. Med. Chem.* **2008**, *16*, 94–99; b) M. Masuko, S. Ohuchi, K. Sode, H. Ohtani, A. Shimadzu, *Nucleic Acids Res.* **2000**, *28*, 34e; c) J. N. Wilson, J. Gao, E. T. Kool. *Tetrahedron* **2007**, *63*, 3427–3433; d) Y. N. Teo, J. N. Wilson, E. T. Kool, *J. Am. Chem. Soc.* **2009**, *131*, 3923–3933; e) H. Kashida, T. Takatsu , K. Sekiguchi , H. Asanuma, *Chem. Eur. J.* **2010**, *16*, 2479–2486.
[21] For the preparation of perylen-3-ylmethanol (**14**), see: M. V. Skorobogatyi, A. A. Pchelintseva, A. L. Petrunina, I. A. Stepanova, V. L. Andronova, G. A. Galegov, A. D. Malakhov, V. A. Korshun, *Tetrahedron* **2006**, *62*, 1279–1287.
[22] J. B. Birks, *Rep. Prog. Phys.* **1975**, *38*, 903–974.
[23] a) C. García-Echeverría, *J. Am. Chem. Soc.* **1994**, *116*, 6031–6032; b) A. Ueno, I. Suzuki, T. Osa, *J. Am. Chem. Soc.* **1989**, *111*, 6391–6397.
[24] K_A was determined, taking in consideration ratios between alternated and eclipse forms calculated by NMR experiments, by least-squares analysis fitting to appropriate equations using *Kaleidagraph 3.5* (Synergy Software, Reading, PA). For model and equation used, see: a) J. W. Park, H. E. Song, S. Y. Lee, *J. Org. Chem.* **2003**, *68*, 7071–7076; b) R. B. Martin, *Chem. Rev.* **1996**, *96*, 3043–3064.
[25] a) M. R. Ghadiri, K. Kobayashi, J. R. Granja, R. K. Chadha, D. E. McRee, *Angew. Chem.* **1995**, *107*, 76–78; *Angew. Chem. Int. Ed. Engl.* **1995**, *34*, 93–95; b) T. D. Clark, J. M. Buriak, K. Kobayashi, M. P. Isler, D. E. McRee, M. R. Ghadiri, *J. Am. Chem. Soc.* **1998**, *120*, 8949–8962.
[26] Homodimerization binding constant of **12c** in CH_3CN was determined to be $1.3\times10^8\,M^{-1}$.
[27] Fluorescence studies of **12c** carried out in milliQ water did not show the appearance of the pyrene excimer-emission band, which suggests that the formation of the corresponding dimer is not possible in water or that the solubility of the peptide is much lower.
[28] Heterodimerization binding constant of $\mathbf{D_{11c/12f}}$ in chloroform was estimated by dilution experiments to be $2.5\times10^9\,M^{-1}$.
[29] Perylene-based CP **12f** present only one band with the typical vibronic structure, so it could not be used for association constant determination through excimer formation, because its characteristic lower energy peak than the monomer emission could not be detected even at high concentration. This was attributed to the short lifetime and low quantum yields of the perylene moiety, which precludes the excimer formation and detection if it is not previously preformed.
[30] Given that pyrene-based CP **11c** does not emit at $\lambda = 449$, 479, and/or 513 nm, and the concentration of the perylene-based CP **12f** was kept constant throughout the titration, the increased fluorescence emission intensity can only be consequence of the FRET process in the heterodimer $\mathbf{D_{11c-12c}}$. Furthermore, addition of 1-pyreneacetic acid to **12f** did not induce any change in its emission intensity, a finding consistent with the absence of the heterodimeric species.
[31] Perylene life times could not be precisely measured in heterodimeric species, owing to the perturbation caused by the presence of other supramolecular entities with similar lifetimes.
[32] Bernard Valeur, *Molecular Fluorescence: Principles and Applications*, Wiley-VCH, Weinheim, **2002**.
[33] A. Rieche, H. Gross, E. Höft, *Chem. Ber.* **1960**, *93*, 88–94.

Received: August 8, 2010
Published online: October 26, 2010

